Natural Resources Canada | Ressources naturelles Canada

GEOLOGICAL SURVEY OF CANADA
OPEN FILE 8952

Modelling seabed disturbance and sediment mobility for the Scotian Shelf bioregion, offshore Nova Scotia

M.Z. Li, Y. Wu, Y. Ma, and Y. Wang

2023

Canada

GEOLOGICAL SURVEY OF CANADA
OPEN FILE 8952

Modelling seabed disturbance and sediment mobility for the Scotian Shelf bioregion, offshore Nova Scotia

M.Z. Li[1], Y. Wu[2], Y. Ma[2], and Y. Wang[2]

[1]Geological Survey of Canada, 1 Challenger Drive, P.O. Box 1006, Dartmouth, Nova Scotia
[2]Fisheries and Oceans Canada, 1 Challenger Drive, P.O. Box 1006, Dartmouth, Nova Scotia

2023

Permanent link: https://doi.org/10.4095/331499

This publication is available for free download through GEOSCAN (https://geoscan.nrcan.gc.ca/).

Recommended citation
Li, M.Z., Wu, Y., Ma, Y., and Wang, Y., 2023. Modelling seabed disturbance and sediment mobility for the Scotian Shelf bioregion, offshore Nova Scotia; Geological Survey of Canada, Open File 8952, 1. zip file. https://doi.org/10.4095/331499

Publications in this series have not been edited; they are released as submitted by the author.

ISSN 2816-7155
ISBN 978-0-660-47746-6
Catalogue No. M183-2/8952E-PDF

Table of Contents

Summary

Ocean surface waves and currents can interact to produce strong seabed shear stress and mobilization of sediments that can significantly impact the seabed stability and benthic habitats on continental shelves. Therefore the knowledge of the magnitude and frequency of seabed disturbance by waves and currents and the resulting mobilization of sediment on continental shelves is critical for the spatial planning and management of Canada's offshore lands. Modelled waves, near-bottom tidal current and circulation current data for a 3-year period were used in a widely applied sediment transport module to simulate the seabed shear stresses and the mobilization of observed sediment grain size for the Scotian Shelf bioregion. The modelling results are presented and analyzed to derive updated understanding of seabed disturbance and sediment mobility on the Scotian Shelf.

The Scotian Shelf is affected by strong waves and tidal currents. Maximum mean significant wave height can reach 2.4 m and maximum mean tidal currents can reach 0.5 $m \cdot s^{-1}$. These waves, currents and/or their interaction cause maximum mean bed shear velocities of 5 – 10 $cm \cdot s^{-1}$. Sediments on the Scotian Shelf can be mobilized by tidal currents at least once during the modelled 3 year period over 28% of the shelf area while waves can mobilize sediments at least once over 60% of the shelf area suggesting much stronger sediment mobilization by waves. Interaction between waves and currents can produce enhanced combined wave-current shear velocity that is capable of mobilizing sediments over 74% of the shelf area.

The spatial variation of the sediment mobilization frequencies by component processes was used to classify the Scotian Shelf into six disturbance types. The seabed disturbance type classification based on near-bed tidal currents and new modelled waves suggests that wave dominant disturbance is predominant accounting for 38.2% of the shelf area. Tide dominant disturbance type accounts for 19.1% of the shelf area, the next highest. In comparison with previous studies using depth-averaged tidal currents, the present study based on near-bottom tidal currents has resulted in reduced sediment mobilization frequency by tidal currents, smaller extent of high mobility areas and significant changes of the spatial pattern of disturbance type distribution on the Scotian Shelf. The universal Seabed Disturbance Index and Sediment Mobility Index have also been applied to quantify the seabed exposure to physical processes and sediment mobilization on the Scotian Shelf by accounting for both the magnitude and frequency of these processes. The applications of these indices provide improved quantification of seabed forcing and sediment mobility for several areas on the Scotian Shelf.

1. Introduction

The impacts on the seafloor exerted by waves and currents and the sediment responses to this forcing directly affect the cost and safety of seabed installations for offshore engineering and resource developments (Cacchione and Drake, 1990; Nittrouer and Wright, 1994). Knowledge of seabed disturbance by oceanographic processes and sediment mobility are also required for habitat classification and for understanding the geo-environment control of habitat distribution (e.g. Connor et al., 2004; Hemer, 2006; Kostylev and Hannah, 2007; Harris and Hughes, 2012). Therefore the knowledge of the magnitude and frequency of seabed disturbance by waves and currents and the resulting mobilization of sediment on continental shelves is critical for the planning, management, and sustainable development of the continental shelves of maritime nations. Numerical modelling is the only effective approach for shelf-wide systematic prediction of the seabed disturbance and sediment mobility.

Several researchers suggested that about 80% of the world's shelves are dominated by waves, and 17% by tidal currents (Walker, 1984; Swift et al., 1986). However, there have been very few quantitative analyses of the percentage of the world's continental shelves on which sediment mobilization occurs, and of the spatial distribution of dominant sediment transport processes. Harris and Coleman (1998) used wave data generated by a global climate model to quantify the mobilization of fine sand on the earth's continental shelves. The first comprehensive shelf-wide calculation was by Porter-Smith et al. (2004) who used wave climatology data for 1997−2000 and tidal model predictions over a spring-neap cycle to separately assess the relative spatial distribution of wave and tide dominated portions of the Australian continental shelf. Their study found that sediments are mobilized by waves on ~31% of the continental shelf and by tidal currents on ~41% of the shelf. Porter-Smith et al. (2004) only considered the frequency of sediment mobilization and did not include a measure of intensity. Their approach also did not consider the effect of the enhanced combined-flow shear stress due to wave and tidal current interaction which would underestimate the bed stress and sediment mobilization frequency. Hemer (2006) evaluated the exposure of the Australian continental shelf to oceanographic processes by modelling the combined wave and current shear stress for an 8-year period incorporating both the intensity and frequency of this parameter. Three methods of classifying the levels of oceanographic exposure were presented. Hemer (2006), however, did not compare the combined-flow shear stress with the threshold of sediment transport, hence the magnitude and frequency of sediment mobilization was not specifically predicted.

In Canada, good efforts have been made to quantify the magnitude and frequency of seabed disturbance, and to use this to understand sediment transport patterns and the distribution and mobility of bedforms for both regional and shelf scales (e.g. Li et al., 2012; Shaw et al., 2014; Li et al., 2015; Li et al., 2021a; Li et al., 2021b). In a modelling study of bed shear stress and seabed disturbance on Sable Island Bank on the outer Scotian Shelf, Li et al. (2012) demonstrated that

tidal currents alone can cause sediment mobilization over 36% of the bank area while wave action affects 71%. The combined action of waves and tides greatly enhances bed shear stress that affects 93% of the bank and mobilizes sediments to water depths as deep as 200 m. Li et al. (2015) applied modelled waves, tidal currents, and wind-driven and circulation currents to simulate seabed shear stresses, sediment mobility and sediment transport patterns in the Bay of Fundy. Seabed shear in the Bay of Fundy is predominantly due to tides, with waves only affecting coastal areas. The strongest mean shear velocity approaches 10 $cm \cdot s^{-1}$ which causes sediment mobilization >30% of the time over most of the bay, often reaching 100% of the time in some areas of the bay. Seabed disturbance and sediment mobility indices incorporating both the magnitude and frequency of these parameters were also proposed and applied to quantify the seabed forcing and sediment mobilization in the Bay of Fundy. In an initial Canada-wide effort, wave hindcast data and modelled tidal current data for a 3-year period were used in a combined-flow sediment transport model to simulate the seabed shear stresses and the mobilization of uniform medium sand by waves and tides on all continental shelves of Canada (Li et al., 2021a). The Canadian continental shelves were found to be impacted by strong waves and tidal currents that produce mean bed shear velocity > 5 $cm \cdot s^{-1}$. The modelling study predicts that medium sand can be mobilized by tidal currents over 36% and by waves over 50% of the shelf area of Canada, while the combined wave-current shear stresses further increase sediment mobilization to over 68% of the shelf area. Quantitative estimates of spatial variation of the relative importance of wave and tidal current disturbances were used to classify the continental shelves of Canada into six disturbance types. Universal Seabed Disturbance (SDI) and Sediment Mobility (SMI) indices were proposed to better quantify the exposure of the seabed to oceanographic processes and sediment mobility incorporating both the magnitude and frequency of these processes. This Canada-wide modelling study thus established the first national framework of seabed disturbance and sediment mobility on the continental shelves of Canada, and was applied by Shaw et al. (2014) in the synthesis of processes, landforms, and benthic habitats on the Canadian Atlantic shelf. The major limitations of this initial national study are that important ocean circulation and storm-driven current processes were not included, and that uniform medium sand instead of observed grain size data was used.

There have been limited applications of seabed disturbance information to the distribution of benthic habitats for Canada's oceans. Kostylev and Hannah (2007) were the first to develop the benthic habitat map for the Scotian Shelf using a disturbance-scope for growth template and readily available oceanographic data. The characteristic combined-flow shear stress was computed based on near-bed tidal currents empirically extrapolated from modelled depth-averaged tidal current data and the 90^{th} percentile of hindcast significant wave height and period data. Thus the disturbance calculation was not computed using time series data of waves and currents and hence likely skewed to the dominance by the extreme wave parameters (see Li et al., 2021a). A disturbance parameter was calculated as the ratio of the total combined wave-tide shear velocity to the critical shear velocity for sediment motion. Their disturbance parameter

therefore only considers the magnitude of the seabed forcing and does not account for how often the disturbance occurs. Gregr et al. (2016) used a similar approach for a habitat classification for the Canadian Pacific continental shelf.

In the latest effort in modelling seabed disturbance for the Canadian continental shelves, Li et al. (2021b) modelled waves, tidal current and circulation current on the Canadian Atlantic Shelf for a 3-year period of 2002 – 2005. Bathymetry and observed sediment grain size data together with the modelled wave and current data are input in a combined-flow sediment transport model to simulate the shear stresses and sediment mobilization by wave, tidal current, circulation current as well as the combined waves and current processes. The modelling results show that observed sediments on the Atlantic Shelf can be mobilized by tidal currents over 30% of the shelf area while storms can mobilize sediments over 35% of the shelf area. Further more, combined-flow shear stress due to wave-current interaction is capable to mobilize sediments over 63% of the shelf area, nearly double that due to either tides or waves. The shelf is also classified into five disturbance types based on the seabed disturbance rate and the relative impact of tidal, wave, and ocean current processes. Universal SDI and SMI indices were also applied to better quantify the exposure of the seabed to oceanographic processes and mobilization of observed sediment grain size incorporating both the magnitude and frequency of these processes. The study by Li et al. (2021b) hence has updated the framework of seabed disturbance and sediment mobility developed in Li et al. (2021a) for the Atlantic Shelf. The key limitations of this modelling study for the Atlantic Shelf are that depth-averaged tidal currents were used, thus over-estimating bed shear stress and sediment mobilization by tides. Also, waves were modelled with relatively coarse spatial resolution which tend to limit the application of the modelling results for focused local studies.

As part of the Marine Geosciences for Marine Spatial Planning (MGMSP) Program (2018-2023), the Geological Survey of Canada-Atlantic (GSCA) is collaborating with DFO to apply the latest wave, current and sediment transport models to estimate bed shear stresses and mobilization of observed sediments on the Scotian Shelf and Newfoundland-Labrador shelves to support the marine spatial planning of these bioregions. In this latest modelling study, a newly developed high resolution 3-D current model is used to predict near-bed tidal and circulation currents. Waves are simulated with a high-resolution wave model. A widely applied sediment transport model is used to estimate not only bed shear stresses but also the sediment transport pathways and spatial patterns of sediment erosion and accumulation for both bioregions. The objectives of this report are (1) to present the modelled waves, currents, and bed shear stress results on the Scotian Shelf, (2) demonstrate the updated framework of the magnitude and frequency of seabed shear stress and sediment mobilization by various processes, (3) derive a classification of the Scotian Shelf based on the modelled spatial variation of the relative importance of wave, tidal and circulation current disturbance, and (4) apply several universal indices for the quantification of seabed disturbance and sediment mobility on the Scotian Shelf,

accounting for both the magnitude and frequency of these processes based on the latest bed shear stress and observed grain size data.

2. Methods

The approach in this study is essentially to apply various wave and current models to derive time series data of waves and near-bed tidal, ocean circulation and wind-driven currents for the period of January 2017 to December 2019 for the Scotian Shelf bioregion (Figure 1). The modelled wave and current data were coupled with bathymetry and updated observed grain size data in a sediment transport model to predict bed shear stresses due to various processes. The computed bed shear stresses were then compared with the critical shear stress for the initiation of sediment motion to quantify the magnitude and frequency of sediment mobilization by wave, tide and ocean circulation processes. Spatial resolutions are quite different among current and wave models, bathymetry, and grain size data. Bathymetry and grain size data therefore were interpolated to the common unstructured grid of the current and wave model (the unstructured mesh shown in Figure 2) for the shear stresses and sediment mobility calculations. This common model domain was defined by 40° to 46°N and 58° to 71°W with a total of 146,812 triangular cells (Figure 2). Figure 1 displays the color-shaded bathymetry of the modelling domain and key geographic locations cited in the report. It should be noted that the model domain shown in Figures 1 and 2 is slightly larger than Scotian Shelf as it includes the US parts of the Gulf of Maine and Georges Bank, and is smaller than the defined Scotian Shelf bioregion (Fisheries and Oceans Canada, 2009) since it does not include the eastern most portion of Scotian Shelf. Therefore the boundaries of Scotian Shelf is defined in very general terms and is used interchangeably with the term of Scotian Shelf bioregion in this report.

2.1 Circulation model

The current model used in this study is the Finite Volume Community Ocean Model (FVCOM; Chen et al., 2003), which is a three-dimensional numerical model based on an unstructured grid system. The model domain (Figure 2) covers the Bay of Fundy, Gulf of Maine, Georges Bank, and the Scotian Shelf. The domain is enclosed by an open boundary in the south that approximately follows the 500 m isobath. Our mesh has a total of 146,812 horizontal triangular cells and 78,715 nodes with grid sizes ranging from 150 m in the nearshore to 10 km on the open shelf (Figure 2). Detailed description of the FVCOM model is given in Feng et al. (2022). The performance of the FVCOM model was verified through comparison of various modelled and observed parameters, and the detailed comparisons between the modeled results and the observations can be found in Feng et al. (2022).

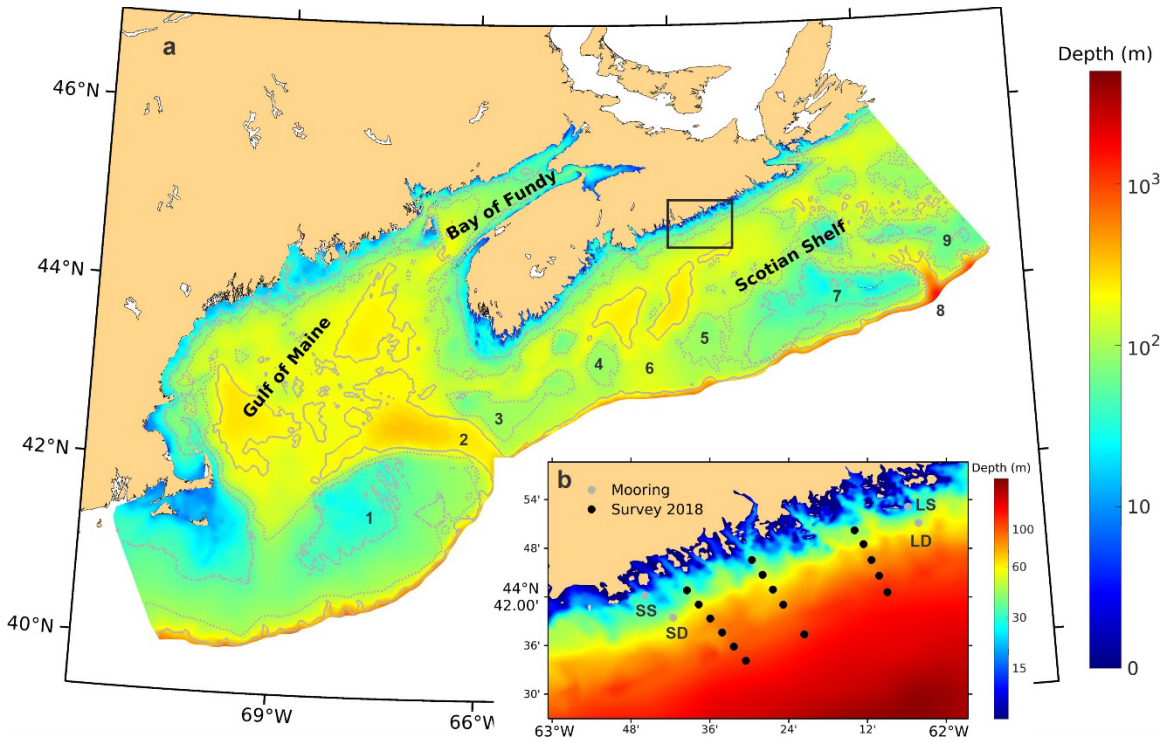

Figure 1 (a) Map of Scotian Shelf showing the shaded bathymetry of the modelling domain and geographic locations. The box marks the Eastern Shore Islands nearshore area that is enlarged in (b). The dashed, dotted, and solid lines mark the isobaths of 50, 100 and 200 m respectively. (b) The bathymetry in the ESI nearshore area. The grey dots indicate the locations of the moored ADCPs. The black dots represent the hydrographic survey sites from 2018 (not used). The numbered places in (a) are 1 Georges Bank, 2 Northeast Channel, 3 Browns Bank, 4 LeHave Bank, 5 Emerald Bank, 6 Scotian Saddle, 7 Sable Island Bank, 8 The Gully, and 9 Banquereau Bank.

The unstructured triangular mesh used by the FVCOM has the advantage of geometric flexibility that provides the ability to better fit the complex coastlines like the archipelago topography of the Eastern Shore Islands region. The insert of Figure 2 indicates that the grid resolution varies smoothly from 150 m to 3 km for the Eastern Shore Islands region. The model was vertically discretized into 45 layers based on a hybrid terrain-following coordinate system which uses the generalized terrain-following coordinate system in depths > 220 m and uniform sigma coordinate system in depths < 220 m. The generalized terrain-following coordinate system consists of 10 layers with z levels at the surface layer, 3 layers with z levels at the bottom, and 32 layers in the middle; the interval of the z levels is 5 m in both the surface and the bottom layers. The benefit of using a terrain-following coordinate system is that the coordinates follow the topography and represent the bottom boundary conditions better, especially in shallow waters of the nearshore and outer-shelf banks.

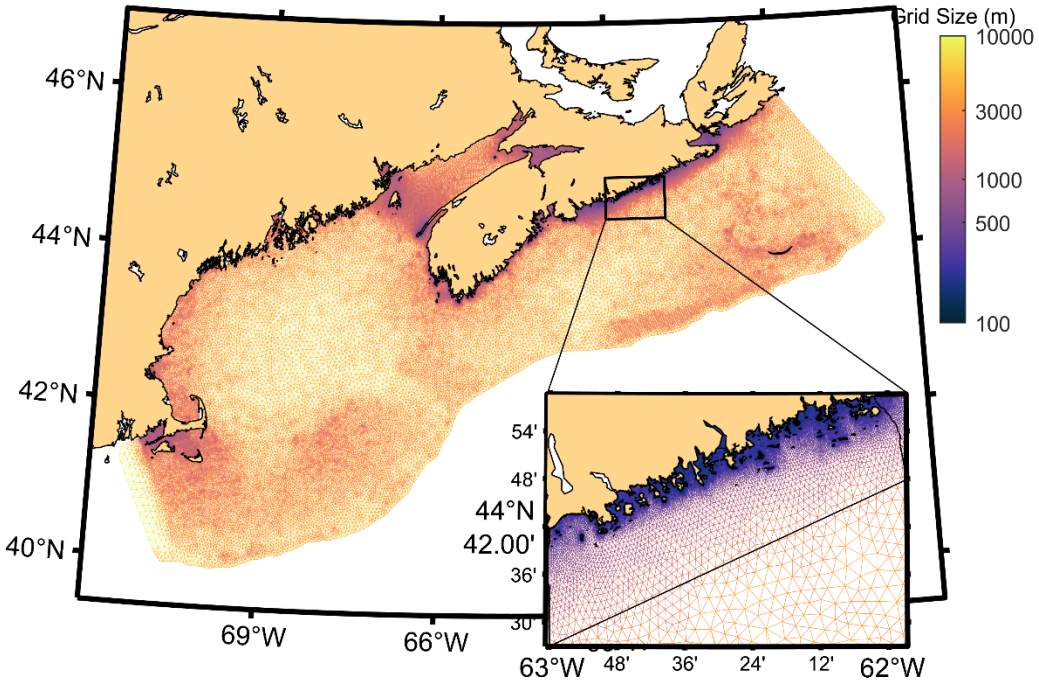

Figure 2 Map of current and wave model domain and mesh size. The insert shows an enlargement of the Eastern Shore Islands (ESI) area.

Surface atmospheric forcing consists of wind at 10 m above the ocean surface, air temperature at 2 m, relative humidity at 2 m, precipitation, evaporation, downward shortwave radiation, and downward longwave radiation. We obtained these forcings with 1/4° resolution from ERA5 reanalysis datasets (https://www.ecmwf.int/en/forecasts/datasets/reanalysis-datasets/era5) from the European Centre for Medium-Range Weather Forecasts. We interpolated the initial and lateral open boundary conditions (excluding tides) from daily-averaged sea surface height, temperature, salinity, and horizontal currents from the global ocean physical reanalysis (GLORYS12V1) with 1/12° resolution. Tidal constituents (M2, S2, N2, O1, K1, P1 and Q1) at the lateral open boundaries were also applied as boundary conditions. The tidal elevations and transports at the open boundaries were obtained from the FES2014 global tidal database which has a resolution of 1/16° (Lyard et al., 2016). Rivers were excluded from our study so the effects of runoff at the coastal boundaries were not included. The model runs through a one-way nesting scheme with values from the global model output described above. The FVCOM model outputted hourly 3D total currents that encompass tidal currents and circulation currents for the period of 2017 – 2019.

The performance of the FVCOM model was verified through comparison of various modelled and observed parameters (details in Feng et al., 2022). We compared the observed with the modelled tidal amplitude and phase of the dominant tidal components (M_2, S_2, N_2, O_1 and

K_1) at 55 tide gauge locations to demonstrate how well the tidal model performs. The error statistics are listed in Table 1. The absolute mean differences for the tidal amplitudes and phases were generally small (e.g., 8.7 cm and 3.3 degrees for M_2). The standard deviation of the differences between the observed and modelled tidal amplitudes accounted for 4.0, 8.2, 9.2, 7.3, and 7.2% of the errors relative to the mean tidal amplitudes for M_2, S_2, N_2, O_1, and K_1, respectively. Overall, the modelled tidal amplitude and phase matched their observed counterparts well.

To examine how well our model simulated the tidal currents through the whole water column, the vertical variation of the modelled and observed tidal current ellipses for three dominant tidal constituents (O_1, K_1 and M_2) is shown in Figure 3 for the four mooring sites in the ESI (locations shown in Figure 1). The modelled semi-major axes of the tidal ellipses agreed well with the observed values for both the diurnal and semi-diurnal tides. As a more quantitative measure, the non-dimensional model performance statistic $\tilde{\gamma}^2$ that combines the amplitude and phase errors into a single quantity (Katavouta et al., 2016) was also calculated and shown in Figure 3. The $\tilde{\gamma}^2$ values are significantly less than 1 indicating that the FVCOM model predicts the observed tidal currents with small error.

Table 1 The absolute mean and standard deviation of the differences between observed and modelled tidal elevation amplitude (ΔA) and phase ($\Delta\phi$) averaged over 55 tide gauges.

Tidal constituents	ΔA (cm)		$\Delta\phi$ (°)	
	Mean	Std	Mean	Std
M_2	8.70	7.61	3.36	3.51
S_2	2.27	2.41	5.23	3.94
N_2	3.35	3.65	6.56	5.50
O_1	1.50	0.71	6.18	3.32
K_1	1.48	0.74	9.80	2.95

2.2 Wave model

The wave model used in this modelling study is the SWAN (Simulating WAves Nearshore) model, which is a state-of-the-art third-generation wave model, especially well-suited for computing wind-generated waves in coastal waters. The model incudes most features of waves in near-shore waters, which cover wave propagation in time and space; wind-generated waves; three- and four-wave interactions; whitecapping, bottom friction and depth-induced breaking,

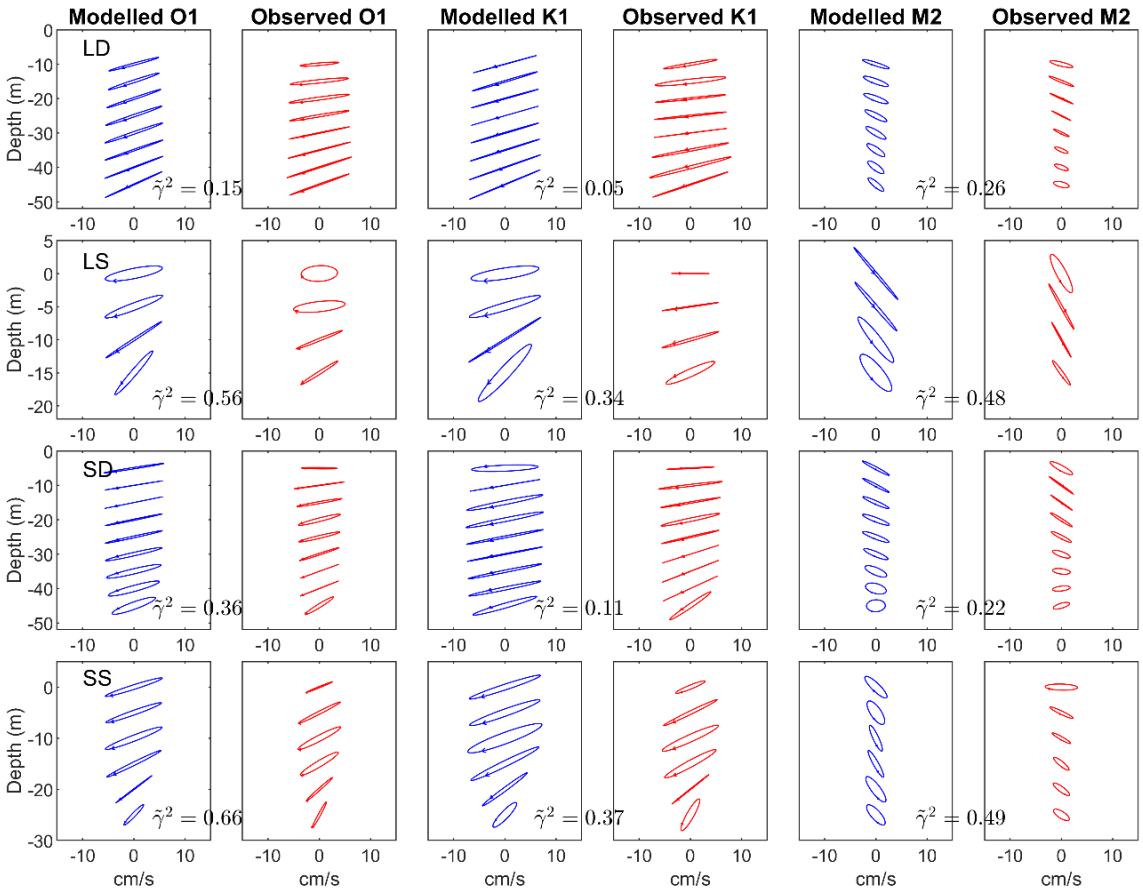

Figure 3 Comparison of modelled (in blue) and observed (in red) O1, K1, and M2 tidal current ellipses based on the vertical profiles of current data collected at the four mooring sites shown in Figure 1b. The values of the depth-averaged non-dimensional model performance statistic $\tilde{\gamma}^2$ (see text for description) are provided.

dissipation due to aquatic vegetation, turbulent flow, viscous fluid mud, and sea ice. The version of WAN 41.31 with the unstructured mesh is used. More details on model equations and model implementations can be found from the website: https://www.tudelft.nl/en/ceg/about-faculty/departments/hydraulic-engineering/sections/environmental-fluid-mechanics/research/swan. The model mesh is the same as that of FVCOM (Figure 2) and the winds used in the wave model are from ERA5 as well. The SWAN model outputs time series data of key wave parameters such as significant wave height, peak wave period, wave propagation direction and bottom wave orbital velocity.

The wave data used for the wave model validation are from eight sites, three nearshore sites (SS, LS and LD shown in Figure 1b) in the ESI area and five sites in relatively open water in the

Gulf of Maine (see Wu, 2021). The simulation period of 2017 – 2019 was selected partly based on the availability of the observational wave data. The time series comparisons between the modelled and the observed significant wave height H_s and peak wave period T_p for the ESI sites are plotted in Figure 4. The comparisons demonstrate that the modelled significant wave heights agree well with the observations, especially at the high wind events, for example, storms in June 2017, October 2018, and August 2019. The correlation coefficients between the model and observation are also shown in Figure 4. For the significant wave height, the correlation coefficients are 0.75, 0.82 and 0.86 for LD in 2017, LS in 2018 and SS in 2019 respectively. All of them are higher than their 95% significant levels. The correlation coefficients for the peak wave periods also indicate that the modelled and observed wave periods are highly correlated although the correlation levels are slightly lower than those of the wave heights. Similarly the scatter plots of the modelled and the observed H_s at the sites in the Gulf of Maine (not shown) gave correlation coefficients mostly higher than 0.82 suggesting high correlation between the model and the observations under open water conditions in the Gulf of Maine. Additional description of the wave model verification can be found in Wu (2021).

2.3 Bathymetry and grain size data

The water column attenuates wave orbital velocity and determines the wave impact on the seafloor. Water depth (bathymetry) is thus an important input for the computation of shear stresses in the bottom boundary layer model. The bathymetry in the FVCOM model was based on high resolution survey data from the Canadian Hydrographic Service with spatial resolutions from 10 meters in the nearshore waters to several kilometers over the open water of the shelf (Wu, 2021). The color-shaded map of the processed bathymetry is presented as the base map in Figure 1. The water depths of the model domain ranges from <10 m in the nearshore to >300 m in channels/gullies and on the upper slope.

Grain sizes of bottom sediment determine the threshold value for the initiation of sediment transport, directly affect the estimates of sediment mobilization level, and also control the values of bottom roughness length which in turn affects the computation of seabed shear stresses. Uniform medium sand was used in the Canada-wide modelling effort of Li et al. (2021a). The more recent seabed disturbance modelling for the Canadian Atlantic Shelf by Li et al. (2021b) used observed grain size data that were largely extracted in June 2008 from the GSC Expedition Database (ED; https://ed.gdr.nrcan.gc.ca/index_e.php) supplemented by additional data (mainly for the Gulf of Maine) obtained from U.S. Geological Survey sediment databases (Reid et al., 2005; Poppe et al., 2014). For the present study, the latest grain size data up to March 2021 have been extracted from ED. The updated observed grain size data also include legacy GSC data that were not initially contained in ED. These are: (1) 279 grain size data from an effort undertaken from 2014−2018 in which legacy samples in the Baffin Bay for which grain

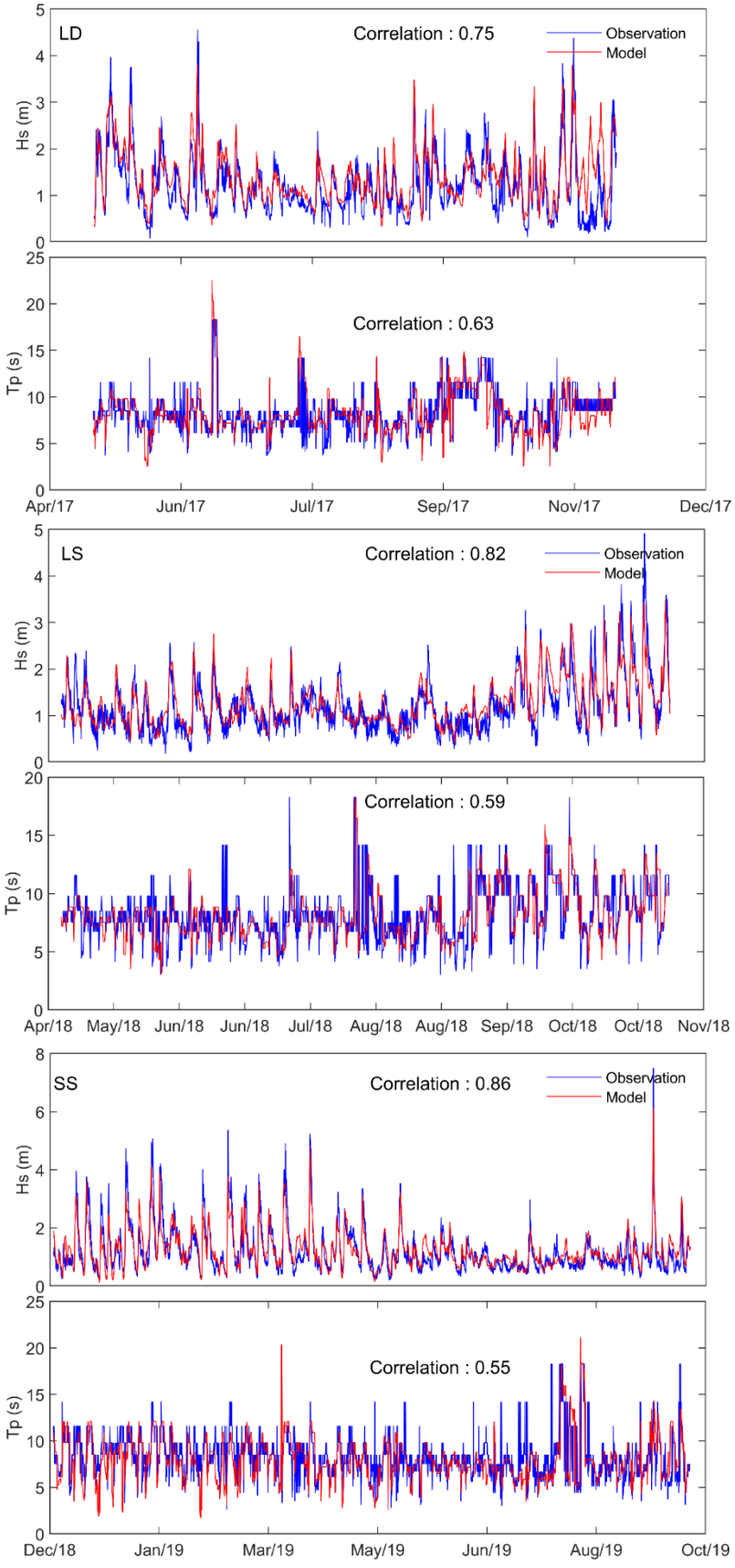
LD
Correlation : 0.75
Observation
Model
Hs (m)
Correlation : 0.63
Tp (s)
Apr/17
Jun/17
Jul/17
Sep/17
Nov/17
Dec/17
LS
Correlation : 0.82
Observation
Model
Hs (m)
Correlation : 0.59
Tp (s)
Apr/18
May/18
Jun/18
Jun/18
Jul/18
Aug/18
Aug/18
Sep/18
Oct/18
Oct/18
Nov/18
SS
Correlation : 0.86
Observation
Model
Hs (m)
Correlation : 0.55
Tp (s)
Dec/18
Jan/19
Mar/19
May/19
Jun/19
Aug/19
Oct/19

Fig. 4 Comparisons of time series of observed (blue) and modelled (red) significant wave height (H_s) and peak wave period (T_p) for 2017 data of site LD (upper 2 panels), 2018 data of site LS (middle 2 panels) and 2019 data of site SS (lower 2 panels). Correlation coefficients are also shown in each panel. See site locations in Figure 1b.

size analysis had not been done in the June 2008 extraction, were strategically selected, retrieved and submitted to GSC Sedlab to obtain grain size data. These 279 grain size data (listed in Appendix 1) includes 131 data from submitted samples processed by SedLab in the 2014−2018 efforts, 92 data that were digitized from another four cruises, and 56 data for Cruise 70037 that were obtained from Dr. John Andrews of University of Colorado (personal communication). (2) 453 data for the Bay of Fundy reported in Long (1979) and 108 data in Baffin Bay reported in OF5409 (Praeg et al., 2007) were also digitized (Appendix 2). (3) An additional 123 data for the Bay of Fundy collected by DFO in the years 1977 and 1994 (Tim Milligan and Paul Hill, personal communication) were also included in this modelling study (Appendix 3). The total number of observed grain size data from GSC was 13131 (Figure 5a) in the present study which represents substantial improvement from the 9947 grain size data of the June 2008 extraction utilized in Li et al. (2021b). USGS data for the Gulf of Maine and outer Bay of Fundy areas included in this study were the same as that described in Li et al (2021b).

The essential quality control (QC) and cleaning steps undertaken in Li et al. (2021b) were also used for cleaning the sample-based grain size data for the Scotian Shelf:

- samples without size class percentages and mean grain size values were removed
- samples with the sum of size class percentage less than 90% were not used
- duplicates with identical latitude and longitude and grain size statistics were eliminated
- data from core intervals deeper than 10 cm below the sediment surface were not used

The combined sample-based grain size data for the Scotian Shelf were brought into Matlab® for gridding. A bi-linear interpolation scheme was used to derive the interpolated grain size value at each modelling grid point that is the average of the adjacent observed grain size data weighted by the inverse distance of these data to the interpolation point. The map of the initially gridded grain size data showed artefact bands due to interpolation using poor data coverage in areas such as southern Scotian slope (Figure 5a). These problems were fixed by inserting hypothetical grain size values based on geology, water depth and the relationship between depth and grain size from adjacent areas with grain size data coverage. Spatially distributed values of 5 phi for upper slope (<1000 m depths) and 6 phi for deeper water were inserted for areas of poor data coverage. The selection of the hypothetical grain size values was hence partially expert driven and partially from observed grain size data in adjacent areas. All the observed grain size data and these inserted hypothetical data were gridded again to generate the gridded observed grain size data for the Scotian Shelf as presented in Figure 5b. Given the adequate coverage of observed grain size data in the Bay of Fundy and on the Scotian Shelf, the gridded grain size shown in Figure 5b can be used with confidence. The gridded grain size map suggests that fine-grained sediments (5 – 8 ϕ, silt and clay) are present in the Gulf of Maine, central inner and middle Scotian Shelf, and the

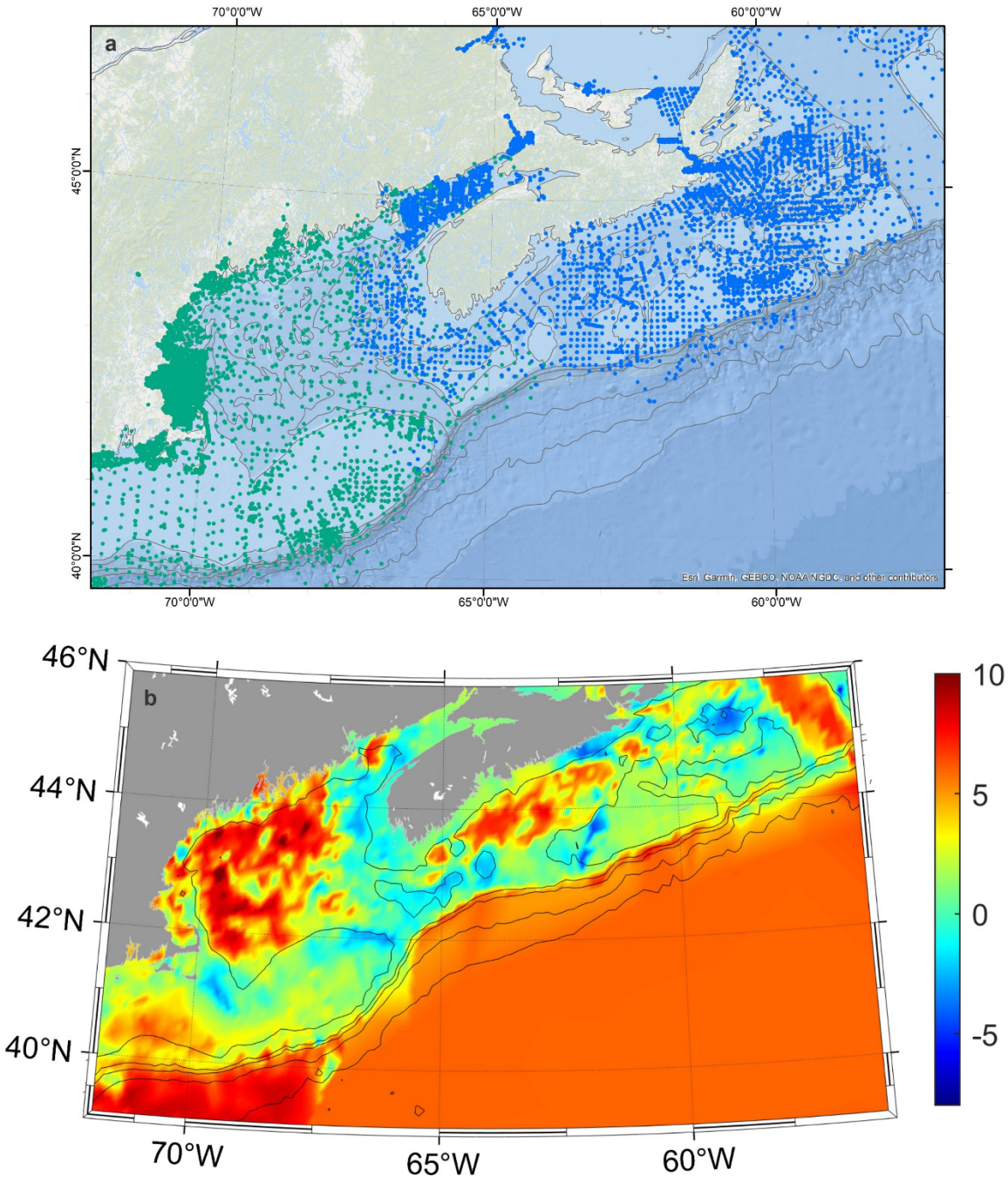

Figure 5 Distribution of (a) sediment samples and (b) gridded grain size data (in ϕ) on the Scotian Shelf. Blue dots are data from GSC ED database and green dots are data from the East Coast Sediment Texture Database and usSEABED database of the USGS. Thin grey lines in (a) represent depth contours of 50, 100, 200, 500, 1000, 2000 and 3000 m. Contour lines in (b) represent depths of 50, 100, 500, 1000 and 2000 m.

Laurentian Channel, while coarser sediments (-1 to -5 ϕ, granules to coarse pebbles) notably occur in the Bay of Fundy, on northern Georges Bank, over western Scotian Shelf and on the western Sable Island Bank. The occurrence of coarser sediments in the Bay of Fundy, on northern Georges Bank, and over western Scotian Shelf shown by the gridded grain size map (Fig. 5b) are in agreement with the mapped distribution of glacial till and gravelly sand in these areas (Fader et al. 1991; Shaw et al. 2012 and 2014). Similarly the distribution of fine-grained Lahave Clay and Emerald Silt materials was mapped for the Gulf of Maine, inner and middle central and eastern Scotian Shelf, and the Laurentian Channel which is well matched by the fine-grained sediments for these areas shown by the gridded grain size map. Therefor patterns of the gridded grain size data are corroborated by the mapped surficial geology (Li et al., 2021a).

2.4 Sediment transport model

The observed surficial sediment grain size data shown in Figure 5b were used in the computation of bed shear stress and sediment transport undertaken in the FVCOM sediment module. This sediment module is essentially that of the ROMS (the Regional Ocean Modeling System) sediment routines that was described in Warner et al. (2008a) and has been applied in numerous modelling studies (e.g. Blaas et al., 2007; Harris, et al., 2008; Warner et al., 2008b; Bever and Harris, 2014). The calculation of bed shear stresses and other bottom boundary parameters under the combined influences of waves and steady currents was quite similar to that of the sediment transport model SEDTRANS (Li and Amos, 2001) utilized in previous seabed disturbance modelling studies (Li et al., 2021a, b). The advantages of the FVCOM sediment module are that it also computes sediment transport pathways as well as the spatial patterns of sediment erosion and deposition on the Scotian Shelf. The ROMS sediment routine is briefly described here with specifics adopted in the present modelling study; see Warner et al. (2008a) for a more detailed description.

Sediment-transport calculations of the sediment module can include sediment settling, resuspension by waves and currents, transport via currents, discharge from rivers, multiple sediment grain classes, and multiple bed layers. The attributes of each sediment class required for the sediment transport calculations include grain diameter, density, settling velocity, critical stress for erosion and deposition, and erosion rate (erodibility coefficient). As the information of percentage of size fractions was not available for many samples, this study only modelled two bed layers - a relatively thin ‘‘active layer’’ sits on top of a vertically uniform substrate layer. The ROMS sediment module accounted for armoring of the seabed by limiting sediment availability within the thin active layer that scaled with excess shear stress and the grain diameter of the sediment on the seabed according to Harris and Wiberg (1997).

The active layer is the interface between water column and sediment bed. The thickness of

the substrate varies over time as the responses to applied shear stress, sediment erosion or deposition. When the bed erodes, substrate sediment is mixed into the active layer. During net deposition the surplus in the active layer from sediment settling is mixed into the substrate. The net sediment exchange between the bottommost layer of the water column and the seabed is the sum of the downward deposition flux, the product of the sediment settling velocity w_s and suspended sediment concentration c (- w_sc), and upward erosion flux E which was calculated following Ariathurai and Arulanandan (1978) as:

$$E_j = E_{0,j} (1- \varphi) f_j (\tau_{sf} / \tau_{cr,j} - 1) \qquad \text{when } \tau_{sf} > \tau_{cr,j}$$

where E_j is the surface erosion mass flux (kg m^{-2} s^{-1}), $E_{0,j}$ is the bed erodibility coefficient (kg m^{-2} s^{-1}), φ (=0.5) is the porosity (volume of voids/total volume) of the top bed layer, f_j is the volumetric fraction of sediment of size class j, τ_{sf} is the skin friction bottom stress attributed to grain size roughness only, $\tau_{cr,j}$ is the critical shear stress for observed sediment grain size specified based on the Shields (1936) diagram and the subscript j is for each sediment class; E_j will be 0 if τ_{sf} is equal to or less than $\tau_{cr,j}$. Sediment settling occurs only when the bed stress is less than the critical shear stress for deposition τ_{cd}. Estimates of net erosion and deposition thicknesses were calculated on the basis of the exchange between the seabed and the water column, adjusted for a porosity of 50%.

As in Li et al. (2021b), both cohesive and non-cohesive sediments were modelled in this modelling study for Scotian Shelf (Table 2). Mean grain size D = 0.024 mm was used to identify the seabed sediments as either cohesive (silt and clay, D ≤ 0.024 mm) or non-cohesive (sand, D > 0.024 mm). Because many samples do not have the information of percentage of size fractions, size class fraction data contained in some samples were not used for the sediment erosion and transport rate computation. The modelled sediment classes together with their attributes of source location (river vs. seabed), sediment type, mean diameter as well as other related hydro-sediment dynamics properties are listed in Table 2. The diameter of medium silt at 0.024 mm was taken as the mean grain size for the cohesive class. The diameter of fine sand at 0.13 mm was taken as the mean grain size for the non-cohesive class. For the cohesive class, the value of τ_{cr} was the same as that of Li et al. (2021b) and was based on the typical range of values found in the literature on cohesive sediment dynamics (e.g. Gust and Morris, 1989; Amos et al., 1996; Amos et al., 1997; Blaas et al., 2007; Harris, et al., 2008; also Dickhudt et al., 2011 for a review). The value of τ_{cd} was the default value recommended by the FVCOM sediment module. For the non-cohesive class, τ_{cr} was computed from the modified Yalin method of Miller et al. (1977) as described by Li and Amos (2001) based on the grain diameter 0.13 mm. The settling velocity of the cohesive class was set according to Harris et al. (2008) and Sherwood et al. (2018) while that for the non-cohesive class was calculated as function of grain diameter according to Gibbs et al. (1971). The erodibility coefficients E_0 were set at $1x10^{-4}$ and $3x10^{-3}$ for the cohesive and non-cohesive classes respectively. These are in agreement with values used in Blaas et al. (2007),

Table 2 Sources, sediment class and type, mean grain size diameter, critical shear stress for erosion τ_{cr}, critical shear stress for deposition τ_{cd}, settling velocity w_s, erodibility coefficient E_0, and fraction of input for the sediment classes used in this modelling study for Scotian Shelf. The last column indicates that the entire layer takes on the same corresponding grain diameter once cohesive or sand sediment types are determined from the spatially variable observed grain size data as presented in Fig. 5.

Sediment Source	Sediment Class	Sediment Type	Diameter (mm)	τ_{cr} (Pa)	τ_{cd} (Pa)	w_s (mm s^{-1})	E_0 kg m^{-2} s^{-1}	Fraction of Input
Seabed	1	cohesive (silt and clay)	0.024	0.15	0.05	0.4	$1x10^{-4}$	100%
Seabed	2	sand	0.13	0.13	-	10	$3x10^{-3}$	100%

Harris et al. (2008) and Warner et al. (2008b). It should be noted that the values of τ_{cr} and w_s for non-cohesive sediments in Table 2 are just initial default values and that ROMS module will calculate these parameters in the model runs using the mean grain diameter of the spatially variable observed grain size data read in from the observed grain size data file.

ROMS sediment module implements one of several bottom boundary layer (bbl) theories to compute bed shear stresses and sediment transport. The present study applied the integrated ssw_bbl method (Warner et al., 2008a) that implements the wave–current BBL model of Madsen (1994) along with moveable bed routines proposed by Wiberg and Harris (1994); Harris and Wiberg (2001). The implementation of the ROMS bbl method requires inputs of speed and direction of various currents (e.g. tidal, circulation and wind-driven) at a near-bed reference elevation z_r, significant wave height H_s or representative wave-orbital velocity amplitude u_b, wave period T, and wave-propagation direction θ. The near-bed tidal, circulation and wind-driven currents from FVCOM, the various wave parameters from SWAN, together with water depth and observed grain size data were input in the ssw_bbl method to compute sediment transport as well as bed shear stresses due to various currents, waves, and the combined wave-current cases. Suspended-sediment transport was calculated by solving the advection–diffusion equation (Warner et al., 2008a). Bedload transport was computed using the formulae of Soulsby and Damgaard (2005) that accounts for combined effects of currents and waves. The description of both suspended-load and bedload transport algorithms can be found in Warner et al. (2008a).

In the final step of sediment mobility computation, the hourly skin-friction shear stress by tidal current, waves, circulation current and combined waves and current as computed above was then compared to the critical shear stress for sediment motion τ_{cr} to determine if sediment mobilization occurs. The number of times that the threshold value was exceeded by various processes was then summed at each grid point over the modelled 3 year period to produce the

threshold exceedance (sediment mobilization frequency in % of time) due to tidal current, waves, circulation and combined wave-current on the Scotian Shelf.

3. Waves

The mean significant wave height and mean spectral peak wave period averaged over the 2017−2019 period are shown in Figures 6a and 6b respectively. The distribution of the significant wave height demonstrates a general pattern of decreasing wave intensity from the east to the west. The strongest waves occur on the open eastern Scotian Shelf where the mean significant wave height values reach 2.4 m. The mean significant wave height decreases to ~2 m on central and western Scotian Shelf and further decreases to <1.5 m in the Bay of Fundy. Mean wave periods are the highest on the inner western Scotian Shelf and in the open waters of the eastern Scotian Shelf reaching 8.8 s and 8.7 s respectively. Mean wave periods are 8.5 s on the central Scotian Shelf, reduce to 8.3 s on Georges Bank and further decrease to less than 7.5 s in the Bay of Fundy.

Maximum significant wave height and maximum wave period seem to show somehow different distribution patterns (Figures 7a and 7b). While still holding the general trend of decreasing values from the east to the west, maximum significant wave heights are the highest and reach 10 m on eastern most Scotian Shelf and over the deep waters of the shelf break and upper slope off the Northeast Channel and the southeastern Georges Bank. Maximum significant wave heights are 8 m on central and western Scotian Shelf and < 6 m in the Bay of Fundy. There are also two areas with low maximum wave heights (< 6 m) at the top of Georges Bank and Sable Island Bank respectively. Maximum wave periods display nearly uniform value of 20 s over the entire Scotian Shelf bioregion.

4. Bottom currents

Currents on the continental shelves can be driven by different oceanographic processes such as tidal currents, mean circulation, and wind-driven currents during storms. Currents caused by these processes can have different magnitudes and spatial patterns, and hence impact the seabed sediments differently. The raw outputs from the FVCOM model are the hourly 3D total currents that encompass tidal currents and circulation currents for the period of 2017 – 2019. T_Tide was used to separate hourly tidal currents from the FVCOM total currents. The remaining total currents with tidal currents subtracted are the total circulation currents (circulation currents hereafter). The total circulation currents represent the vectorial sum of the background mean circulation current and the instantaneous wind-induced current during storms. The circulation currents have been vector averaged to derive the mean (residual) circulation currents and the mean circulation currents have then been vectorially subtracted from the total circulation currents to derive the storm-driven currents. The magnitude and spatial distribution patterns of near-

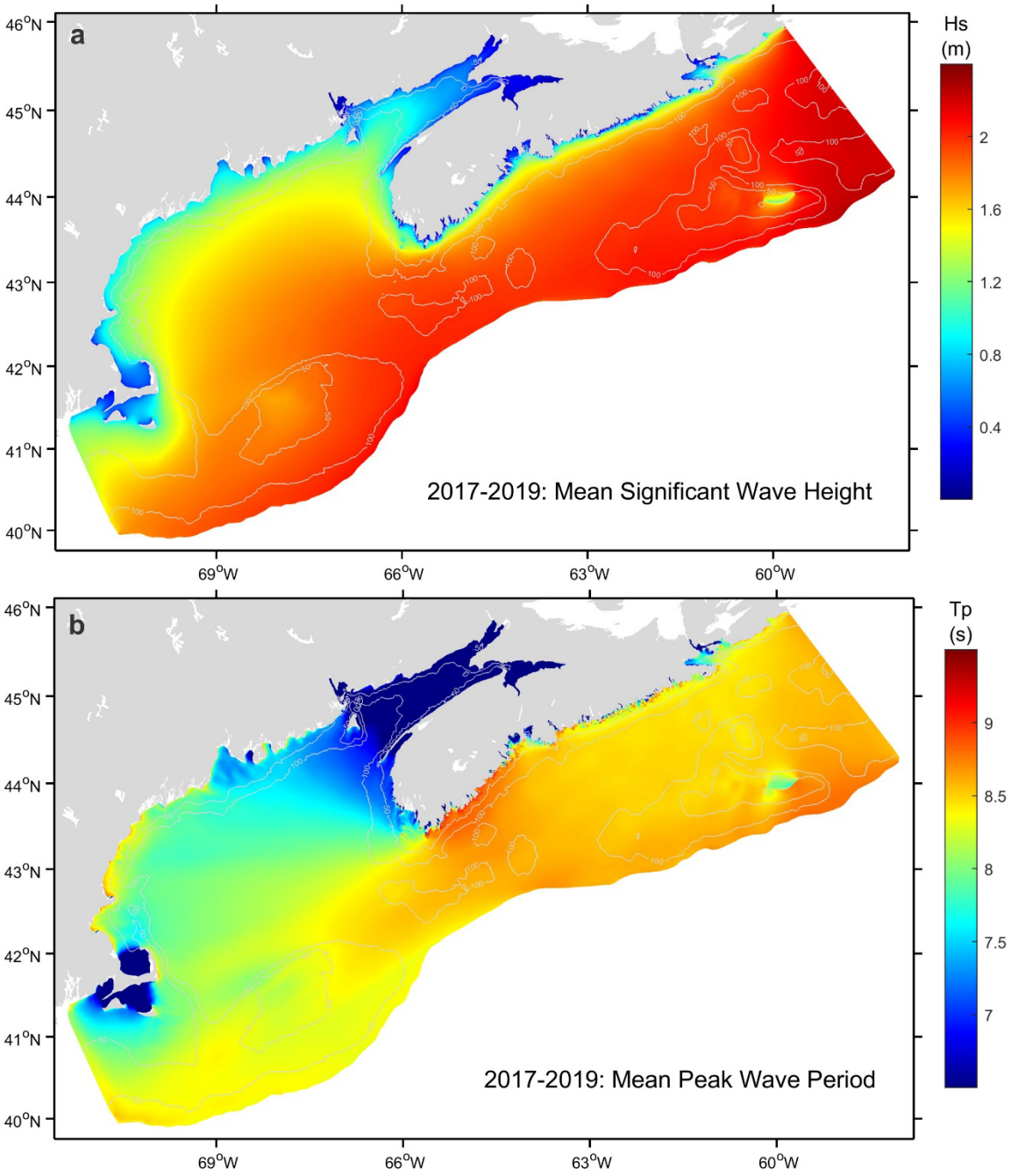

Figure 6 Spatial distribution of (a) mean significant wave height (H_s) and (b) mean spectral peak wave period (T_p) on the Scotian Shelf averaged over the modelled period of 2017 – 2019.

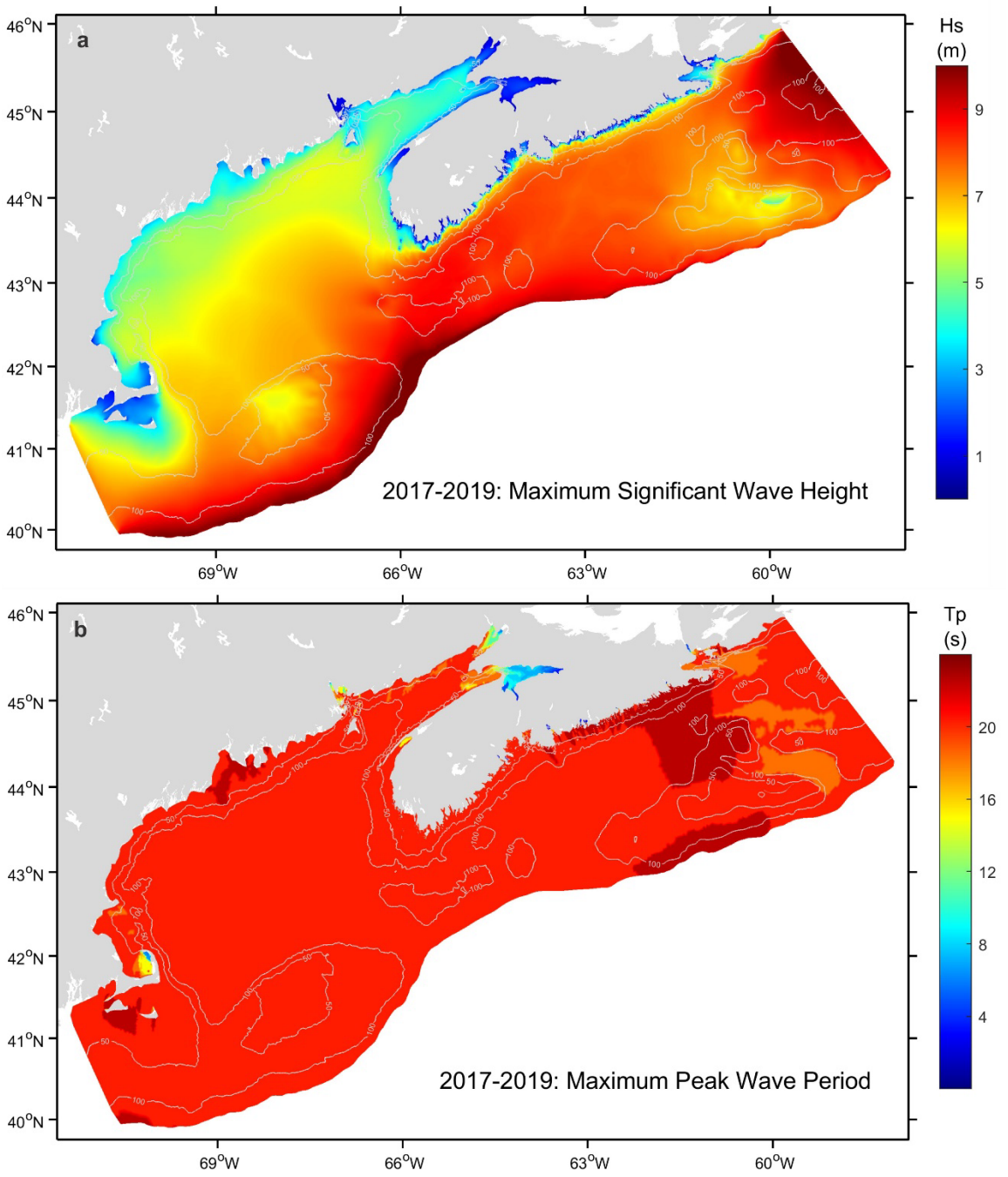

Figure 7 Spatial distribution of (a) maximum significant wave height (H_s) and (b) maximum spectral peak wave period (T_p) on the Scotian Shelf over the period of 2017 – 2019.

bottom tidal currents, circulation currents and storm-driven currents are presented in this section. The relative magnitudes and spatial variation of the seabed impact by these currents are also summarized.

4.1 Tidal currents

Mean and 95th percentile near-bed tidal current speed are respectively presented in Figures 8a and 8b; the latter gives a measure of the extreme conditions of the tidal currents. The highest mean tidal currents on the Scotian Shelf occur in the upper Bay of Fundy where the speeds are > 0.5 m·s^{-1}. Strong tidal currents of 0.4 − 0.5 m·s^{-1} are found in the Bay of Fundy, on the inner and mid-Scotian Shelf off southwestern Nova Scotia, and on Georges Bank. Moderately high tidal currents of 0.3 m·s^{-1} are predicted on western Browns Bank and in the Northeast Channel. Low to moderate tidal currents of 0.1 – 0.2 m·s^{-1} are found for the banks on the outer Scotian Shelf. Tidal currents are low (<0.05 m·s^{-1}) over the remaining areas of the Scotian Shelf, particularly over the Gulf of Maine and in the basins behind the outer shelf banks. Edge effects can be found at the southwest and northeast boundaries of the model domain (e.g. Fig. 8) for speeds of tidal, circulation and storm-driven currents and their corresponding shear velocity and sediment mobilization frequency (presented in various maps in sections below). The edge effects are mainly due to the interpolation of currents, temperature and salinity in the nesting zone, which are from the global model of Glorys with the temporal scale of daily, in contrast to the hourly of the model results in the inside of the model domain.

The distribution pattern of the 95th percentile tidal current speed is nearly identical to the mean tidal current speed. However the values are on average 50 to 100% higher largely reflecting the changes of current speed between peak flood/ebb and high/low slack tides and that between neap and spring tides. For instance, the speed increased from 0.4 m·s^{-1} of the mean tidal current to 0.7 m·s^{-1} of the 95th percentile tidal current speed on Georges Bank. The mean tidal currents are 0.2 m·s^{-1} on Sable Island Bank and the 95th percentile tidal current speed increases to 0.4 m·s^{-1}. As indicated in Li et al. (2021b), these strong spatial variations of tidal current speed are attributed to either the distribution of tidal ranges or the effect of tidal resonance. The significant change of strong tidal currents in the Bay of Fundy and on Georges Bank and western Scotian Shelf, to low and moderate speeds on the central and eastern Scotian Shelf is due to a combination of different tidal ranges, Georges Bank being a part of the Gulf of Maine - Bay of Fundy tidal resonance system (Garrett 1972) and Georges Bank causing topographic acceleration of the tidal flow (Li et al., 2021a, b).

4.2 Circulation currents

The hourly near-bottom total circulation currents were used to compute the mean and 95th percentile near-bottom circulation current speed for the modelled 3 year period. These are respectively presented in Figures 9a and 9b. Several differences from the distribution of tidal current stand out. Firstly, the magnitude of circulation currents is significantly less than that of the tidal currents and largely is less than 0.2 m·s^{-1} except for the upper Bay of Fundy and along the shelf edge of the Gully where the mean circulation currents reach > 0.3 m·s^{-1}. Secondly,

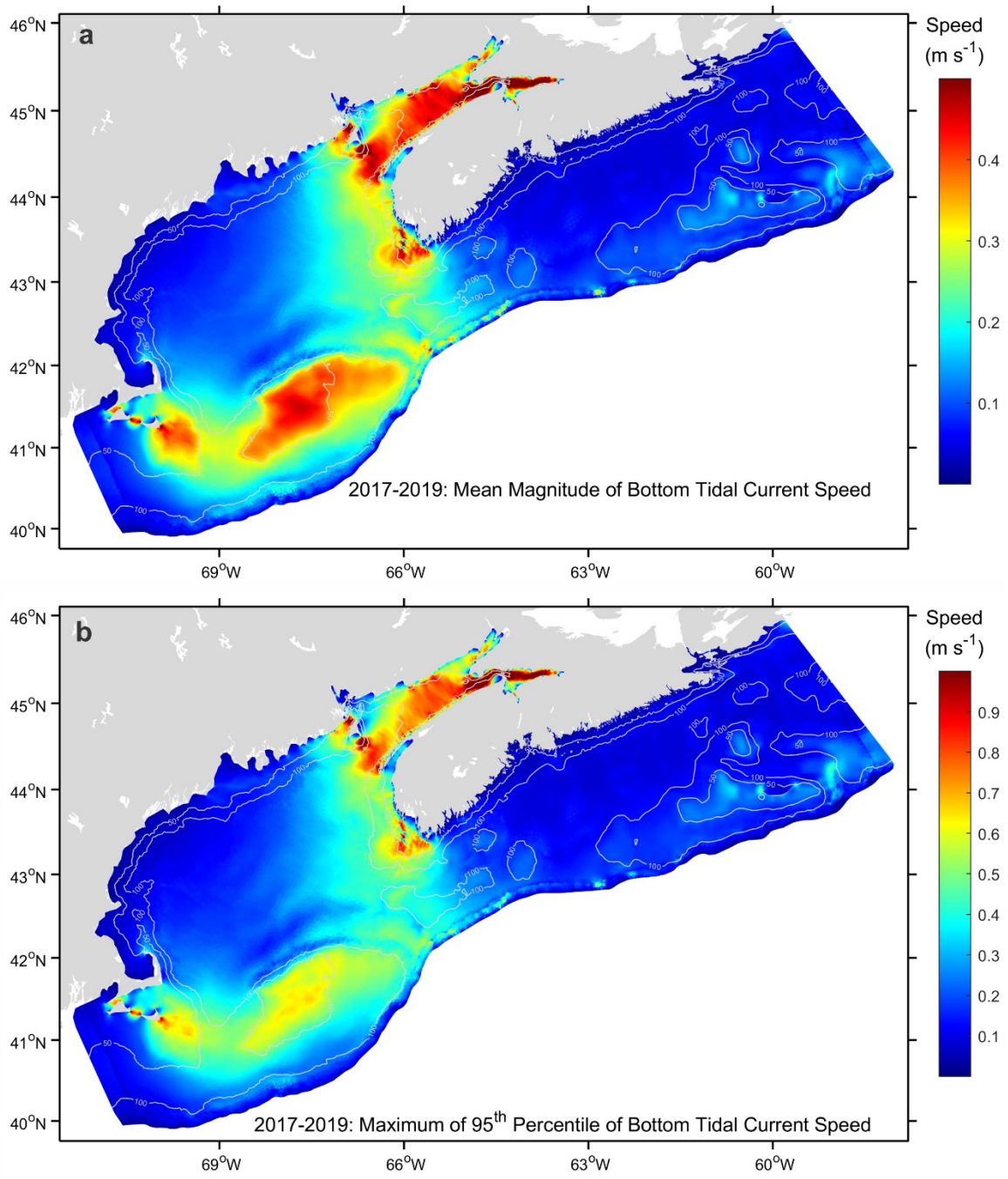

Figure 8 Spatial distribution of (a) mean and (b) 95th percentile near-bed tidal current speed on the Scotian Shelf over the period of 2017 – 2019.

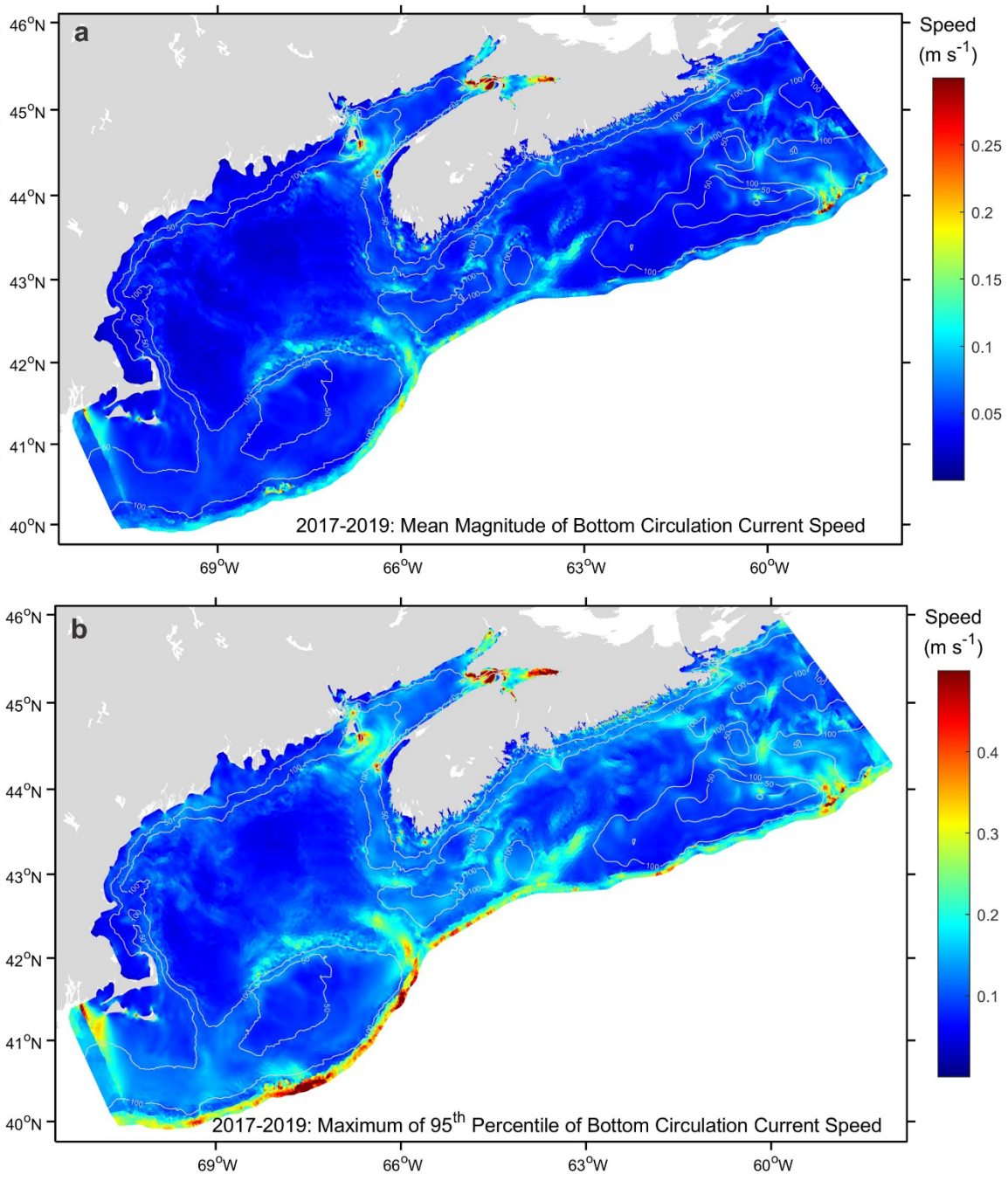

Figure 9 Spatial distribution of (a) mean and (b) 95th percentile near-bed circulation current speed on the Scotian Shelf over the period of 2017 – 2019.

moderate to strong tidal currents widely occur in the Bay of Fundy and on other areas on the shelf (Figure 8a) while circulation currents are minimal in these areas (except for patches in the upper Bay of Fundy). The moderate circulation flows of 0.2 – 0.3 $m \cdot s^{-1}$ are concentrated in narrow belts along the shelf edge and upper slope and in deeper channels (e.g. Northeast Channel, the Scotian Saddle between LeHave and Emerald Banks, and the Gully). The spatial distribution of the 95th percentile circulation current speed in Figure 9b shows essentially the same patterns as the mean circulation currents. However, the peak values moderately increase to ~0.5 $m \cdot s^{-1}$ particularly in the upper Bay of Fundy, along the shelf edge off eastern and southern Georges Bank, and along the shelf edge of the Gully.

4.3 Storm-driven and total currents

The distribution of the 95th percentile storm-driven currents is presented in Figure 10. The main feature is that winds during storms introduce additional near-bed currents up to ~0.3 $m \cdot s^{-1}$ in magnitude mainly in the upper Bay of Fundy and along the shelf edge and upper slope. Moderate storm-driven currents of 0.2 $m \cdot s^{-1}$ also occur in cross-shelf channels and in patches on the outer-shelf banks.

Mean and 95th percentile total current speed are respectively presented in Figures 11a and 11b. The highest mean total currents on the Scotian Shelf reach > 0.5 $m \cdot s^{-1}$ and occur in Bay of Fundy. Strong mean total currents of 0.4 $m \cdot s^{-1}$ are found on Georges Bank and on the inner and mid-shelf off southwestern Nova Scotia. Moderate total currents of 0.3 $m \cdot s^{-1}$ are predicted on Browns Bank and in the Northeast Channel. Low to moderate total currents of ~0.2 $m \cdot s^{-1}$ are found for the banks on the outer Scotian Shelf. Total currents are low (<0.1 $m \cdot s^{-1}$) over the remaining areas of the Scotian Shelf. The magnitude and spatial patterns of the total currents are thus quite similar to that of the tidal currents shown in Figure 8a. The magnitude of the mean total currents is only slightly higher than the mean tidal currents. The main difference, however, is that since the total currents include the contribution of the circulation current, Figure11a hence also demonstrates the presence of narrow belts of moderate flows of 0.2 – 0.3 $m \cdot s^{-1}$ along the edge and upper slope of the Scotian Shelf. The 95th percentile total current (Figure 11b) demonstrates nearly identical patterns to the mean total currents. However, the maximum values increased to 1 $m \cdot s^{-1}$ in the Bay of Fundy while the moderate currents on Georges Bank increase to 0.6 – 0.7 $m \cdot s^{-1}$. These represent ~50% increases over the mean total currents suggesting the importance of extreme values of the total currents in assessing the intensity and frequency of seabed disturbance.

4.4 Magnitude and distribution of various current processes

The relative magnitudes and spatial distribution patterns of various currents for the Canadian Atlantic Shelf were evaluated by Li et al. (2021b). Since the near-bottom tidal currents have been modelled in the present study, the magnitude and distribution patterns of the near-bottom tidal,

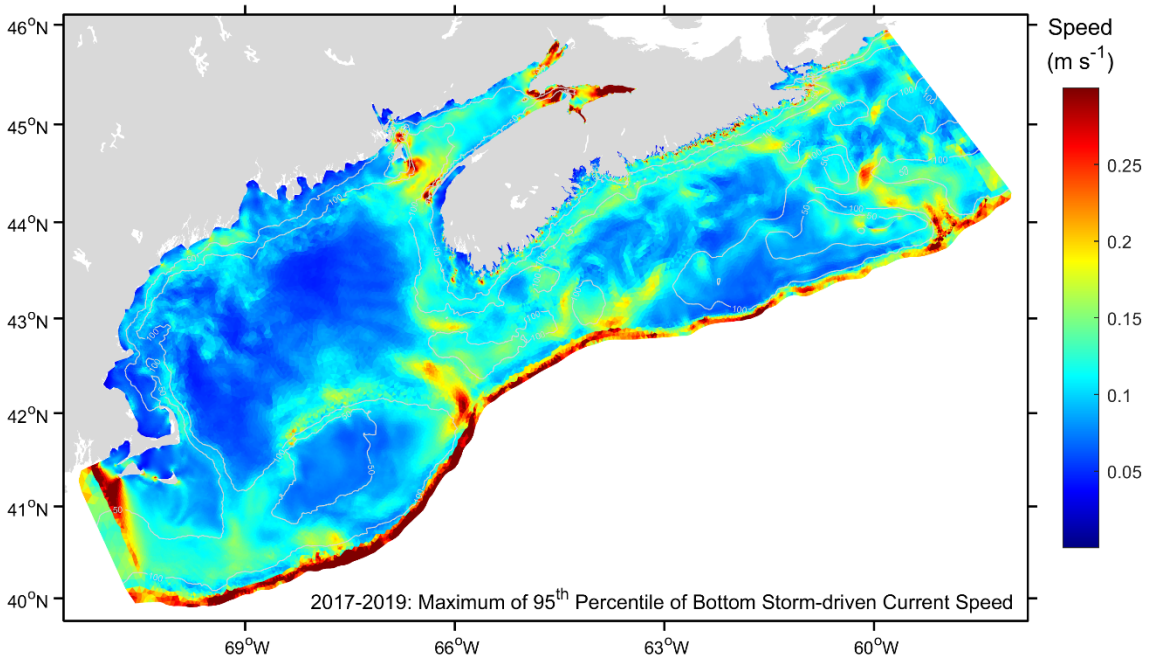

Figure 10 Spatial distribution of 95th percentile near-bed storm-driven current speed on the Scotian Shelf over the period of 2017 – 2019.

circulation, storm-driven and the total currents on the Scotian Shelf can now be more adequately assessed.

The magnitude and spatial distribution of the near-bottom tidal, circulation, and storm-driven currents presented in Figs. 8, 9, and 10 respectively, demonstrate while circulation and 95th percentile storm-driven currents have similar magnitudes of 0.2–0.3 m·s^{-1}, the maximum mean tidal current speeds reach >0.5 m·s^{-1}. Tidal currents are thus the predominant current component on the Scotian Shelf. The impact of circulation currents is essentially confined along the perimeters over the shelf edge and upper slope. The effects of the storm-driven currents widely occur on the open shelf. Although the impact of the tidal currents is also distributed widely on the open shelf, their greatest impact occurs in the Bay of Fundy and western Scotian Shelf and decrease significantly on the central and eastern Scotian Shelf. With the exception of the presence of moderate total currents along the shelf edge and upper slope (Figure 11), the magnitude of the total currents is only slightly higher than the tidal currents (Figure 8) and the spatial distribution of the mean total currents are essentially the same as that of the mean tidal currents. This comparability implies that averaged over the modelled 3 years, the vectorial addition of the storm-driven and the circulation currents causes insignificant changes to the magnitude of the total currents which were used in the computation of the combined wave-current shear stress.

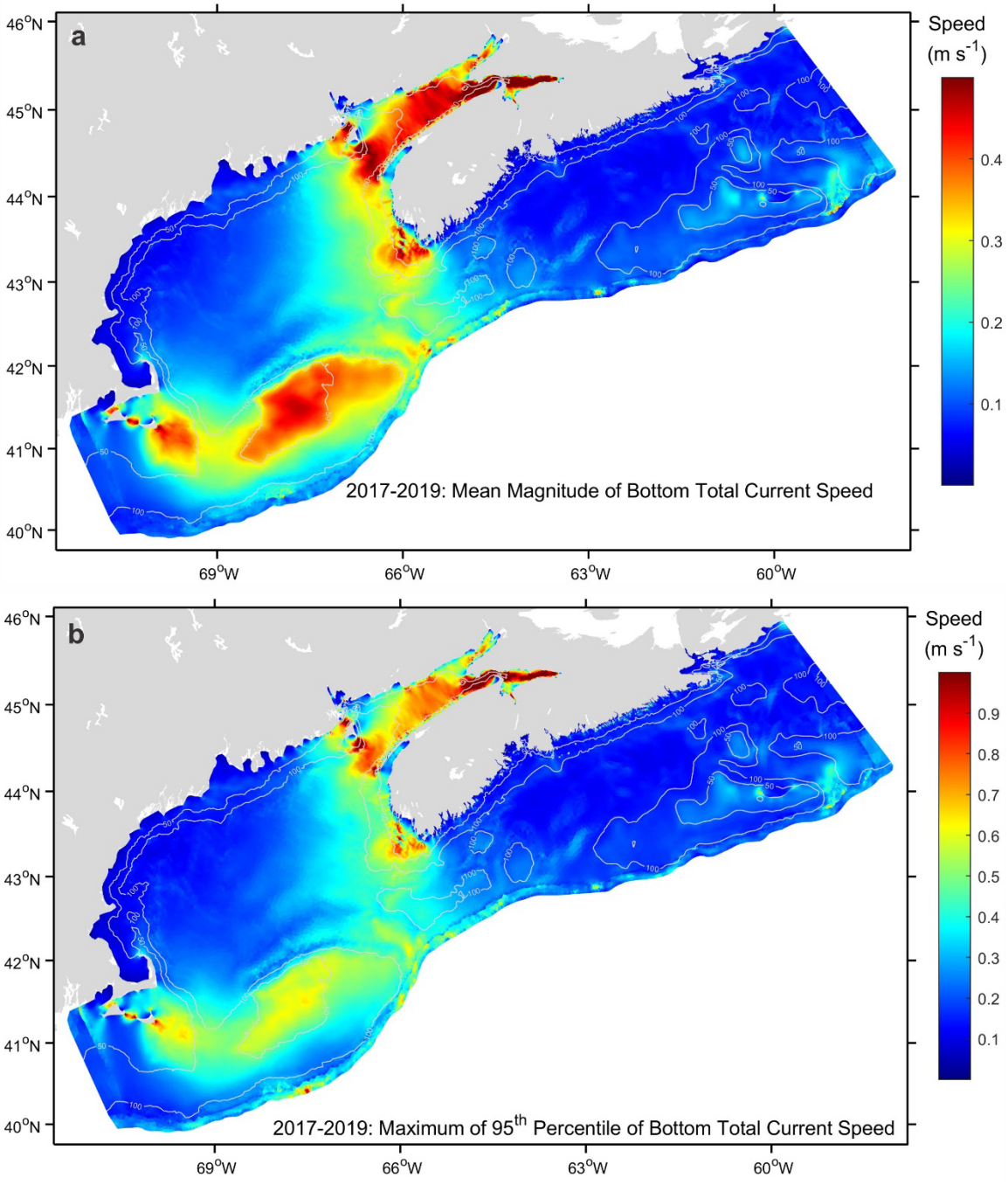

Figure 11 Spatial distribution of (a) mean and (b) 95th percentile near-bed total current speed on the Scotian Shelf over the period of 2017 – 2019.

5 Seabed shear stress and sediment mobilization

The magnitude and spatial distribution of mean and 95th percentile shear velocity and the sediment mobilization frequency due to individual component processes of tides, waves, and circulation currents are first presented. These are followed by presenting the distribution of the shear velocity and sediment mobilization frequency by the combined waves and currents to demonstrate the overall spatial patterns of seabed forcing and sediment mobility under the combined effects of individual oceanographic processes.

5.1 Sediment mobilization by waves

The mean significant wave height presented in Figures 6a demonstrates a general trend of decreasing wave intensity from the east to the west. The wave impact on the seafloor, however, strongly depends on the water depths rather than the distribution of wave heights on the ocean surface. Mean wave shear velocity in Figure 12a demonstrates that the strong waves on the open eastern Scotian Shelf and over the deeper waters of East Channel (Figure 6a) do not translate to strong impact at the seabed due to the deep water depths in these areas. Wave impact on the seabed is generally restricted in shallower waters on the outer shelf banks and along the coasts. The spatial distribution of the mean wave shear velocity (Figure 12) shows that the strongest wave shear velocity of ≥ 2 cm·s^{-1} occurs on Georges Bank, Sable Island Bank and along the coasts. Low to moderate mean shear velocity of 0.2 – 0.7 cm·s^{-1} are predicted on Browns Bank, LeHave Bank and Banquereau Bank. Wave impact on the seabed is minimal over the vast remaining areas of Scotian Shelf.

Extreme values of shear stresses from various processes not only represent the potential maximum force exerted on the seabed by each process but also determine if sediment mobilization occurs or not. Therefore the spatial distributions of the 95th percentile wave shear velocity is presented in Figures 12b. As storms occur on the intermittent frequency (2 to several days) and are seasonally stronger in the winter, the extreme values of the wave shear velocity represented by the 95th percentile wave shear velocity (Figure 12b) are greatly different from the mean values averaged over multiple years (Figure 12a). The maximum values of the 95th percentile values on the Scotian Shelf are nearly double of the mean values. For instance, the mean wave shear velocities of ~2 cm·s^{-1} increase to ~4 cm·s^{-1}on the Georges and Sable Island Banks. The impact areas of the 95th percentile wave shear velocity also increase substantially; the wave shear velocity >0.3 cm·s^{-1} affects approximately 70% of the Scotian Shelf.

The percentage of time that waves alone cause mobilization of observed grain sizes on the Scotian Shelf is presented in Figure 12c. The map of wave sediment mobilization frequency shows overall patterns very similar to that of the mean wave shear velocity of Figure 12a.

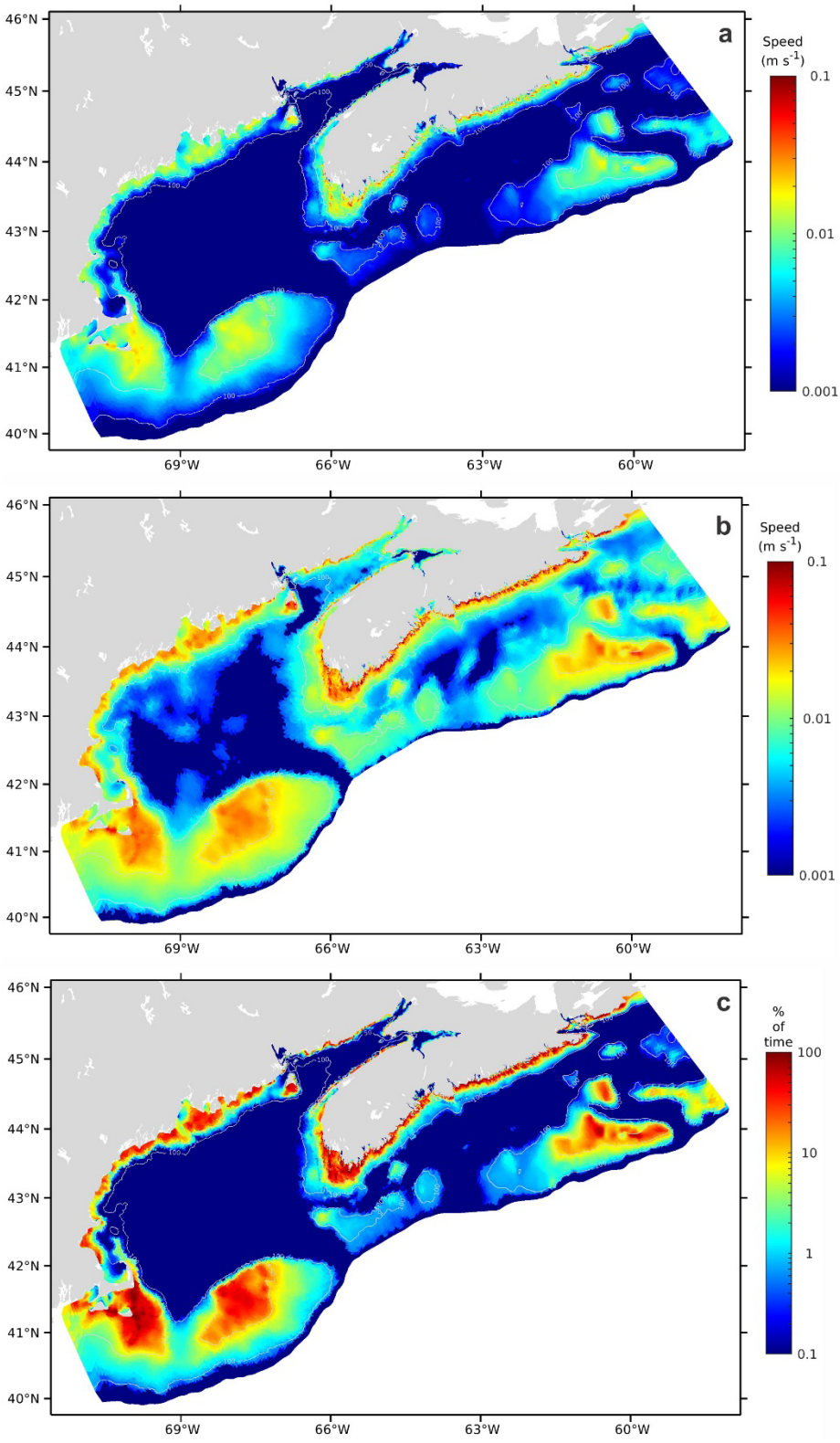

Figures 12 Spatial distribution of (a) mean wave shear velocity, (b) 95th percentile wave shear velocity, and (c) sediment mobilization frequency (% of time) by waves on the Scotian Shelf over the period of 2017 – 2019.

The highest wave mobilization frequency, greater than 50% of the time, occurs over patches on Sable Island Bank and on the inner shelf off southwestern Nova Scotia. Moderately high frequency of wave mobilization of 30–50% is found over Georges Bank and along the coasts of Nova Scotia. Low to moderate mobilization frequency of 5 − 10% occurs on western Browns Bank and the Banquereau Bank. Low mobilization frequency of 0.5 − 2% are found on the remaining areas of Browns Bank, on LeHave and Emerald Banks, and over mid-shelf patches on the western and eastern Scotian Shelf. Waves alone do not cause sediment mobilization over the vast areas of Bay of Fundy, the Gulf of Maine and the basins behind the outer shelf banks.

The percentage of shelf area over which various processes exceed the threshold of sediment motion can be used to quantify the relative importance of component processes in the mobilization of observed sediments on the Scotian Shelf. The shelf break often occurs in water depths down to 300–500 m over the northern parts of the Atlantic Shelf (Piper, 1991). Li et al. (2021b) hence used the depth range of 10 – 500 m to define the total area of the Atlantic Shelf. The shelf break on the Scotian Shelf is approximately at 200 m depth (Piper, 1991; Shaw et al., 2014). The mesh of the FVCOM current model for Scotian Shelf used in this study (Feng et al., 2022) extends into waters much shallower than 10 m. Therefore the depth range of 5 – 200 m was used to define the total area of the Scotian Shelf at ~169 x 10^3 km^2. The wave threshold exceedance data have been used to compute the area and the percentage of shelf area over which waves exceed the threshold of sediment motion at least once over the modelled 3 year period. These statistics are listed in Table 3. Figure 12c together with Table 3 demonstrate that waves are capable of mobilizing sediments at least once over 60.4% of the Scotian Shelf area.

Table 3 Area and percentage of total shelf area of threshold exceedance of observed grain sizes by the processes of tides, waves, circulation current and combined waves and current on the Scotian Shelf.

Processes	Total shelf area (km^2)	Area (km^2)	% of shelf area
	168,737		
Tide		47,327	28.0
Wave		101,936	60.4
Circulation		41,227	24.4
Combine wave-current		124,708	73.9

5.2 Sediment mobilization by tidal currents

In contrast to the restricted distribution of wave shear stress, the impact of tidal current shear velocity occurs widely on the Scotian Shelf. The patterns of the mean tidal current shear velocity (Figure 13a) are well correlated with that of the mean tidal current speed (Figure 8a). The highest

mean tidal current shear velocity occurs in the upper Bay of Fundy and reaches ~5 $cm \cdot s^{-1}$. These are significantly higher than the maximum values of the mean wave shear velocity on the Scotian Shelf shown in Figure 12a. The impact of the tidal currents also has a much broader distribution as the moderately high values of mean tidal shear velocity (2 – 3 $cm \cdot s^{-1}$) widely occur in the Bay of Fundy, on Georges Bank and on western Scotian Shelf. Low to moderate mean tidal current shear velocity of 0.5 – 1.5 $cm \cdot s^{-1}$ are found on several outer shelf banks.

As tidal processes are dominated by the semidiurnal frequency, the 95th percentile tidal current shear velocity (Figure 13b) does not present drastic changes from the mean values. The maximum tidal current shear velocity only increases from 4 − 5 $cm \cdot s^{-1}$ of the mean shear velocity to 7–8 $cm \cdot s^{-1}$ as the 95th percentile values. These moderate increases in the magnitude and spatial impact range should largely come from the variations of the neap-spring cycles at the fortnightly frequency.

The percentage of time that the tidal current alone causes mobilization of observed sediments on the Scotian Shelf is presented in Figure 13c. It is immediately clear that sediment mobilization by tidal currents has higher intensity than that of waves and that sediment mobilization by tidal currents are predominantly confined to the Bay of Fundy, western Scotian Shelf and Georges Bank while that by waves are dominantly on the outer shelf banks such as Georges Bank and Sable Island Bank (see Figure 12c). The highest frequency, 50 − 100% of the time, occurs in the Bay of Fundy, on Georges Bank, and on the shelf off southwestern Nova Scotia. Low to moderate mobilization frequencies of 5 – 20% are found on Browns Bank and in patches on Sable Island Bank. Tidal currents cause low mobilization frequencies of 1 – 5% on the Banquereau Bank. Tidal currents do not cause mobilization of observed sediments over the vast remaining areas of Scotian Shelf. The percentage of shelf area over which tidal currents exceed the threshold of sediment motion at least once over the modelled 3 year period is just 28% (Table 3), significantly smaller than the waves.

5.3 Sediment mobilization by circulation currents

The shear velocity of the circulation current (Figure 14a) demonstrates patterns that are yet different from the wave and tidal current shear velocities. Except in the upper Bay of Fundy where mean circulation current shear velocity reaches moderately high values of 2 – 3 $cm \cdot s^{-1}$, the values of mean circulation current shear velocity are generally <0.5 $cm \cdot s^{-1}$ which are substantially lower than that of waves and tidal currents. These low values of circulation current shear velocity are restricted to the perimeters over the shelf edge and upper slope with minimal impact over the vast interior areas of the shelves. Circulation currents represent the background mean ocean currents and vary mainly in seasonal and inter-annual cycles. Therefore the comparison of the 95th percentile and mean circulation current shear velocities (Figures 14a, b) indicates that the spatial distribution patterns of the extreme and mean values are nearly the same

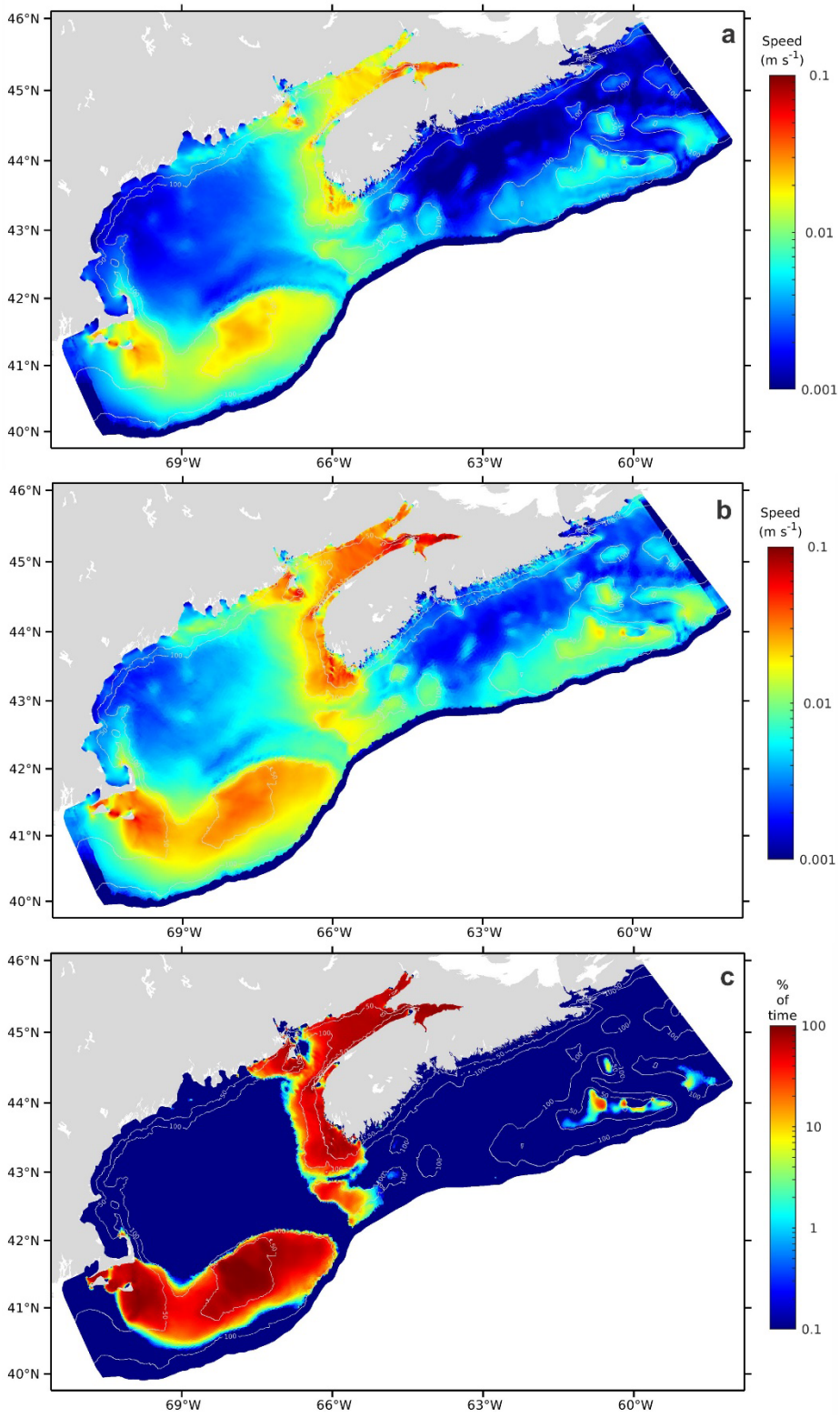

Figure 13 Spatial distribution of (a) mean tidal current shear velocity, (b) 95th percentile tidal current shear velocity, and (c) sediment mobilization frequency (% of time) by tides on the Scotian Shelf over the period of 2017 – 2019.

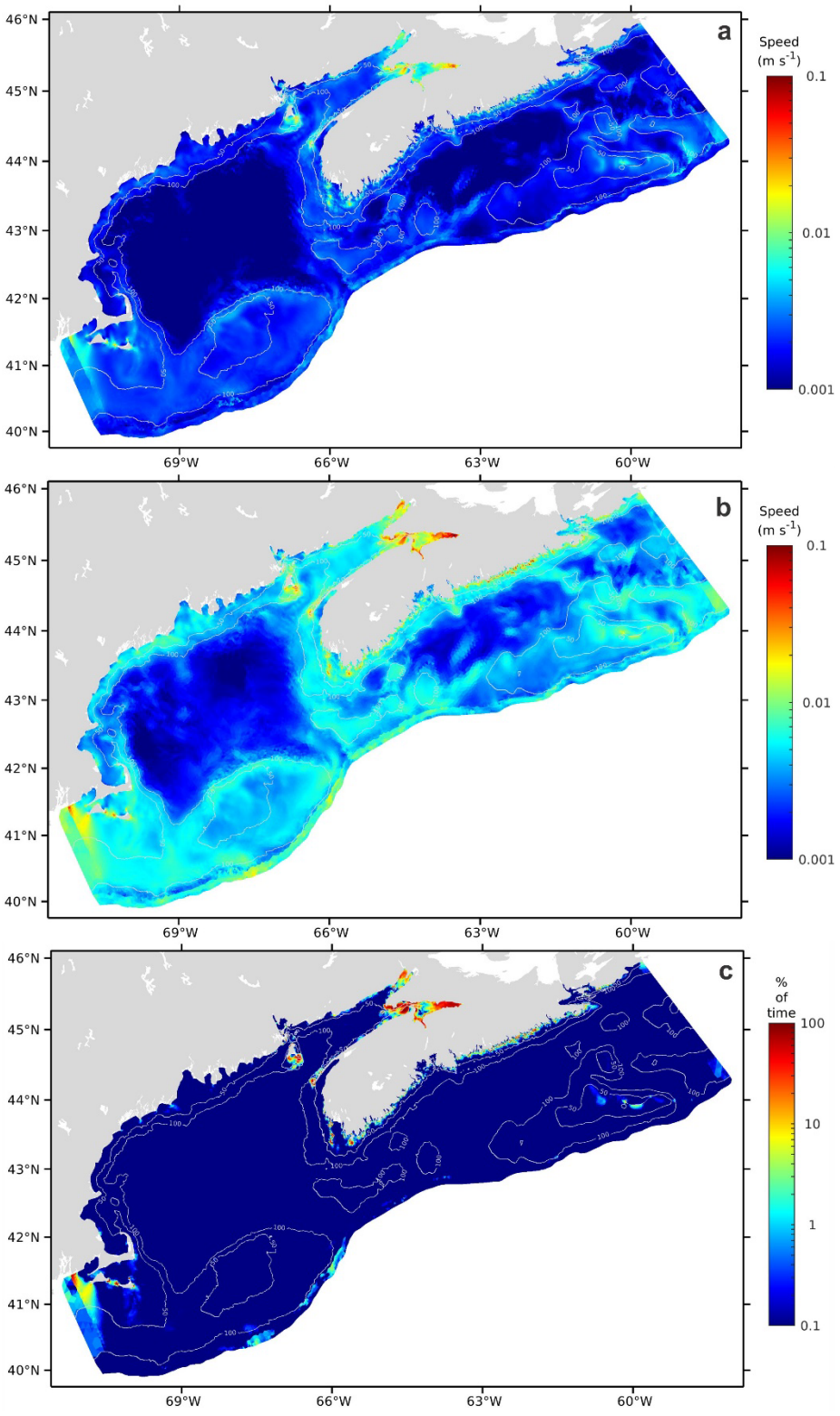

Figure 14 Spatial distribution of (a) mean circulation current shear velocity, (b) 95th percentile circulation current shear velocity, and (c) sediment mobilization frequency (% of time) by circulation current on the Scotian Shelf over the period of 2017 – 2019.

and that only the magnitude increases moderately from ~0.5 cm·s^{-1} of the mean condition to ~2 cm·s^{-1} of the extreme condition.

The percentage of time of mobilization of observed sediments by circulation current on the Scotian Shelf is shown in Figure 14c. The spatial pattern is strongly dependent on the distribution of the circulation current shear velocity presented in Figure 14a. The moderately high mean shear velocity in the upper Bay of Fundy cause moderately high to high (50−70% of time) mobilization in that area. Otherwise minimal (<1%) and low (1 – 10%) mobilization frequency is limited to the shelf edge and upper slope off Georges Bank and western Scotian Shelf, and small patches on Sable Island Bank and Banquereau Bank. The percentage of shelf area over which circulation currents exceed the threshold of sediment motion at least once over the modelled 3 year period is surprisingly high at 24.4% (Table 3) suggesting that shelf area wise circulation currents are equally important as the tidal process in mobilizing sediments on Scotian Shelf.

5.4 Sediment mobilization by combined waves and currents

The mean shear velocity due to the combined wave and total current shown in Figure 15a represents the overall patterns of seabed forcing from integrating all oceanographic processes (tidal currents, waves and circulation currents). The strongest combined wave-current shear velocity is up to 5 – 10 cm·s^{-1} and occurs in the upper Bay of Fundy predominantly due to the energetic tidal currents there. Moderately high combined shear velocity of 3 – 4 cm·s^{-1} is found in the mid-Bay of Fundy, on the shelf off southwestern Nova Scotia, on Georges Bank, and along the coasts of Nova Scotia. Moderate shear velocities of 1–2 cm·s^{-1} are predicted on major outer shelf banks such as Browns Bank, Sable Island Bank and Banquereau Bank. Low shear velocities of 0.5–1 cm·s^{-1} can be found in eastern Gulf of Maine and on other banks on the outer Scotian Shelf. Notable areas with minimal values of combined shear velocity (<0.5 cm·s^{-1}) occur in central and western Gulf of Maine and over the inner to middle Scotian Shelf.

The patterns of the 95th percentile combined wave and current shear velocity (Figure 15b) reflect the effect of the spatial variation of the relative impact of tides and storms. For areas where wave impact is dominant, the values of the 95th percentile combined shear velocity increase by a factor of 2 from the mean values. For instance, the combined shear velocity increases from the mean values of 2 cm·s^{-1} to 4−5 cm·s^{-1} on Sable Island Bank. For areas dominated by tidal processes such as on Georges Bank, the values increase only moderately from ~3 cm·s^{-1} of the mean values to ~4 cm·s^{-1} of the 95th percentile for these areas. Although the spatial patterns of the 95th percentile combined shear velocity are similar to that of the mean, the spatial extent of the impact of the 95th percentile values increases substantially. This is particularly apparent over the Gulf of Maine, western Scotian Shelf, and the outer-shelf of the eastern Scotian Shelf.

The percentage of time that the combined wave-current shear stress causes mobilization of observed sediments on the Scotian Shelf is presented in Figure 15c. The highest mobilization frequency of ~100% of the time occurs in the Bay of Fundy, on Georges Bank, over southwestern Scotian Shelf, and at the top of Sable Island Bank. High mobilization frequency of 50 – 70% is found on western Browns Bank, over the remaining areas of Sable Island Bank, and along the coast of Nova Scotia. Moderate mobilization of 10–20% of the time is predicted in the Northeast Channel and on Banquereau Bank. Low mobilization of 1–10% of the time is found on other outer-shelf banks and over patches on the middle Eastern Scotian Shelf. The combined wave-current shear is minimal and causes no sediment mobilization in the Gulf of Maine and on the inner and middle Scotian Shelf. The improved spatial resolution of the models used in the present study reveals contrast local variation patterns of the sediment mobilization intensity for different regions. Due to the relatively homogenous tidal current distribution in the Bay of Fundy, the spatial pattern of sediment mobilization frequency is largely uniform in that area. On the contrary, sediment mobilization frequency demonstrates strong dependence on water depths on the major banks such as Georges Bank and Sable Island Bank. Mobilization frequency is high or very high (50−70%) on the top of the banks, decreases to moderately high (30−50%) on the mid-banks and is reduced further to low intensity (1−10%) over the deeper waters of 70 – 100 m on the these banks.

Comparison of sediment mobilization frequency by the combined wave-current shear stress (Figure 15c) with that by waves (Figure 12c) and by tidal currents (Figure 13c) clearly indicates that the enhanced shear velocity due to non-linear interaction of waves and currents causes higher frequency and broader distribution of sediment mobilization on the Scotian Shelf. The estimates of areas and % of shelf area in Table 3 show that the combined wave-current shear velocity can mobilize observed sediments at least once over 74% of the Scotian Shelf area for the modelled 3 year period. This is 22% more than that by waves and more than double that by tidal currents.

Since the mean combined wave-current shear velocity in Figure 15a and the sediment mobilization frequency in Figure 15c represent the overall patterns of seabed forcing and sediment mobility from integrating all oceanographic processes, it is thus useful to explore the correlation between combined wave-current shear stress and the sediment mobilization by this shear stress and how grain size variation regionally affects this correlation. The distribution of the sediment mobilization frequency (Figure 15c) demonstrates close correlation with the magnitude of the combined wave-current shear velocity shown in Figure 15a. The highest mobilization frequency in the upper Bay of Fundy, on Georges Bank, and over southwestern Scotian Shelf, are respectively in agreement with the high and moderately high shear velocities over these areas. The occurrence of the minimal values of combined shear velocity in the western Gulf of Maine and on the inner to middle Scotian Shelf also correlates well with the minimal or no sediment mobilization in these areas. Spatial variation of observed grain size, however, causes

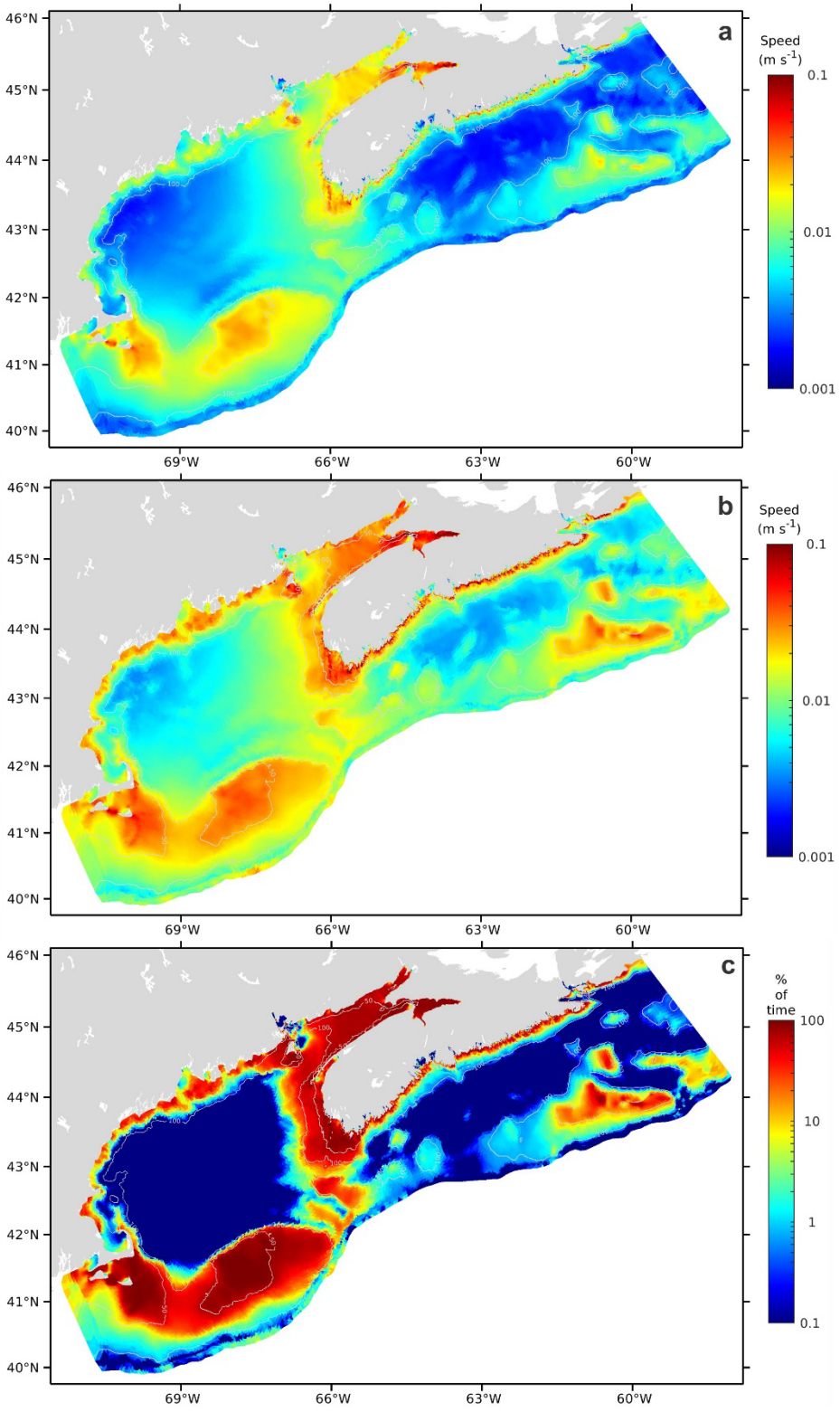

Figure 15 Spatial distribution of (a) mean combined wave-current shear velocity, (b) 95th percentile combined wave-current shear velocity, and (c) sediment mobilization frequency (% of time) by combined waves and current on the Scotian Shelf over the period of 2017 – 2019.

substantial difference in the distribution of the sediment mobilization frequency than that of shear velocity for some areas. The combined shear velocity shows similar moderately high values of 3 – 4 cm·s^{-1} in the middle Bay of Fundy and on Georges Bank (Figure 15a). Sediments in the middle Bay of Fundy, however, are very coarse sand and granules (0 to -1 ϕ) and coarser than the fine to medium sand (~2 ϕ) on Georges Bank (Figure 5b). Therefore sediment mobilization frequency on Georges Bank reaches the highest value of 100% of the time while that in the middle Bay of Fundy is 50 – 70% of the time (Figure 15c). Similarly moderate shear velocities of 1–2 cm·s^{-1} are predicted for both Browns Bank and Sable Island Bank. However, Sable Island Bank is dominated by fine to medium sands while sediments on Browns Bank are dominantly very coarse sand. This difference in grain size renders that sediment mobilization frequency on Sable Island Bank is moderately higher (up to 100%) than on Browns Bank (maximum 50%).

6. Discussion

6.1 Disturbance type classification and statistics

The percentage of shelf area over which various processes exceed the threshold of sediment motion has been used in Section 5 to quantify the relative importance of component processes in the mobilization of observed sediments on the Scotian Shelf. For uniform medium sand, Li et al. (2021a) show that the Atlantic shelf is dominated by wave mobilization as waves can mobilize medium sand over 49% of the shelf area and tidal mobilization only occurs over 34% of the shelf area on the Atlantic Shelf. With the more realistic observed grain size, Li et al. (2021b) find that the shelf areas of sediment mobilization by waves and tides are nearly the same (~30%) on the Atlantic Shelf. The present study for Scotian Shelf used modelled near-bottom currents as well as observed grain size. The modelling results for the 2017−19 duration demonstrates that waves are capable of mobilizing sediments at least once over 60.4% of the Scotian Shelf area while that by tidal currents is only 28% of the shelf area (Table 3).

According to the approach of Porter-Smith et al. (2004) and Li et al. (2015, 2021a), continental shelves can also be classified into disturbance types (i.e. regionalisation) based on quantitative estimates of the spatial variation of the relative importance of threshold exceedance by each component wave, tide and circulation current processes. Such classification delineates what oceanographic process is important to mobilize sediments on different areas of the shelf and also has implications for the distribution of specific benthic habitats (Porter-Smith et al., 2004; Harris and Hughes, 2012). Considering the mobilization frequency of these component processes at each grid point, five disturbance types are defined: (1) unaffected: time% of mobilization by individual wave, tide, and circulation process is all 0; (2) wave dominant: time% of exceedance by wave is at least 3 times that either by tide or circulation current; (3) tide dominant: time% of exceedance by tide is at least 3 times of either wave or circulation current;

(4) circulation dominant: time% of mobilization by circulation current is at least 3 times of either wave or tidal current; (5) mixed disturbance: cases that do not fall into neither of the above four types. The spatial distribution of the seabed disturbance types is presented in Figure 16a and the statistics of the areas and percentages of shelf areas for the five disturbance types are given in Table 4.

The seabed disturbance type classification on the Scotian Shelf based on the relative mobilization frequency of component processes suggests that wave dominant disturbance is predominant accounting for 38.2% of the shelf area and mainly occurs on western central Scotian Shelf and eastern Scotian Shelf, along the coasts of Scotian Shelf, along the coasts of Gulf of Maine, and over the southern margin of Georges Bank. Tide dominant disturbance type is second important to account for 19.1% of the shelf area, only half of the wave dominant type. Tide dominant disturbance mainly occurs in the Bay of Fundy, on Georges Bank and on western Scotian Shelf. Mixed disturbance accounts for only 6.4% of the shelf area and primarily occurs in the upper Bay of Fundy, on the inner shelf off western Nova Scotia, in a patch atop Georges Bank and in a narrow band on the southern Georges Bank. Circulation dominant disturbance type is even less significant (only 0.7% of the shelf area) and is restricted to a patch in the outer Northeast Channel and narrow bands along the edge of eastern and southeastern Georges Bank. Waves, tides and circulation processes alone cause zero sediment mobilization (unaffected type) over 36% of the shelf area (Table 4), predominantly in the Gulf of Maine and in the basins on the inner and middle Scotian Shelf behind the outer shelf banks.

This latest round of modelling using 3D current models and new modelled waves for the period 2017−19 have resulted in several key changes of disturbance type distribution on the Scotian Shelf in comparison with the Atlantic Shelf modelling of Li et al. (2021b) (compare Figure 16a and Figure 16b). The modelling results of Li et al. (2021b) in Figure 16b suggest that the disturbance on Scotian Shelf is predominantly tide dominant while the present modelling study demonstrates the area of wave dominant disturbance to be double that of tide dominant type (Figure 16a and Table 4). Li et al. (2021b) also shows that Georges Bank and the shelf off southwestern Nova Scotia are entirely tide dominant type and that the mid- and outer shelves of the central and eastern Scotian Shelf show mixed wave dominant, tide dominant, and mixed disturbance types. The present modelling study, however, suggests that patches of wave dominant and mixed disturbance types also occur in the former area and the latter area is mostly wave dominant with only very small patches of mixed and tide dominant disturbance types. The shelf area% of disturbance types for the Scotian Shelf from the present study is compared with that for the whole Atlantic Shelf of Li et al. (2021b) and the Australia Shelf presented by Porter-Smith et al. (2004) in Table 5 to put the classification for Scotian Shelf in context of continental shelf scale distribution. Albeit differences in processes modelled and the depth limits for shelf definition, Table 5 suggests that seabed disturbance is predominantly due to waves on the Scotian Shelf while disturbances by waves and tidal currents are equally important when the

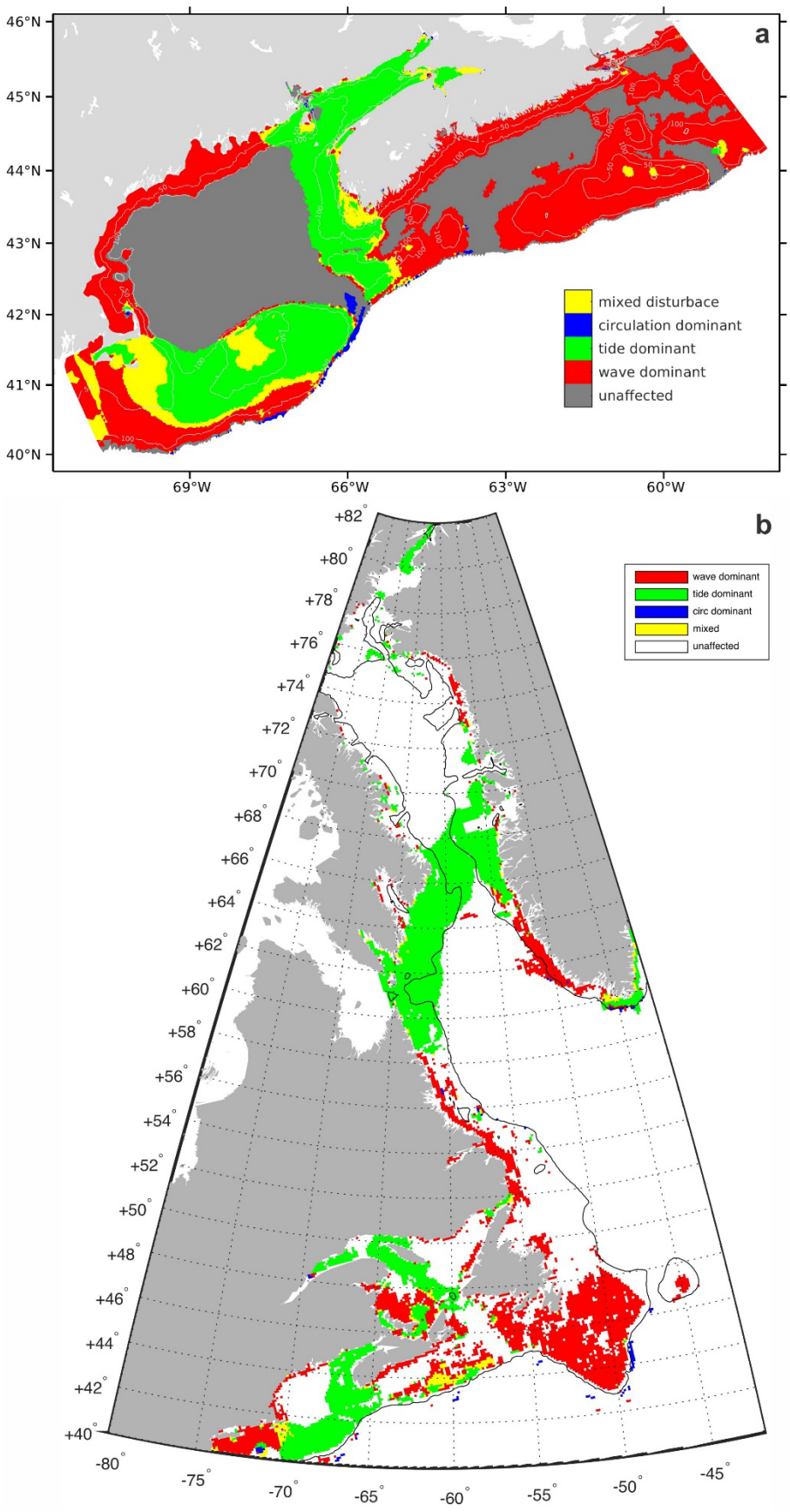
a
46°N
45°N
44°N
43°N
42°N
41°N
40°N
69°W
66°W
63°W
60°W
mixed disturbace
circulation dominant
tide dominant
wave dominant
unaffected
b
wave dominant
tide dominant
circ dominant
mixed
unaffected
+82°
+80°
+78°
+76°
+74°
+72°
+70°
+68°
+66°
+64°
+62°
+60°
+58°
+56°
+54°
+52°
+50°
+48°
+46°
+44°
+42°
+40°
-80°
-75°
-70°
-65°
-60°
-55°
-50°
-45°

Figure 16 Spatial distribution of seabed disturbance types on (a) the Scotian Shelf based on near-bottom tidal current for 2017-19 from this study and (b) the Atlantic Shelf based on depth-averaged tidal currents for 2002-05 from Li et al. (2021b).

Table 4 Area and percentage of total shelf area of various disturbance types on the Scotian Shelf.

Disturbance Types	Total shelf area (km^2)	Area (km^2)	% of shelf area
	168,737		
Tide dominant		32231	19.1
Wave dominant		64432	38.2
Circulation dominant		1,127	0.7
Mixed disturbance		10,764	6.4
Unaffected		60,185	35.7

Table 5 Modelled shelf area percentages of seabed disturbance types for the Scotian Shelf (the present study), the whole Atlantic Shelf (Li et al., 2021b) and the Australia Shelf (Porter-Smith et al., 2004).

Disturbance Types	Scotian Shelf	Atlantic Shelf	Australia shelf
	% of shelf	% of shelf	% of shelf
Tide dominant	19.1	24.6	40.8
Wave dominant	38.2	24.7	30.7
Circulation dominant	0.7	0.1	-
Mixed disturbance	6.4	3.2	1.9
Unaffected	35.7	47.4	26.6

entire Atlantic Shelf is considered. In contrast, seabed disturbance is dominated by tidal currents on the Australia Shelf. Due to relatively deeper water depths and deeper shelf break limit used for the Atlantic Shelf modelling study, shelf area percentage unaffected by individual oceanographic processes is significantly higher on the whole Atlantic Shelf (47%) than the Scotian Shelf (36%). In comparison, the unaffected shelf area% on the Australia Shelf is only 27% suggesting that the individual processes mobilize sediments over much wider proportion on the Australia Shelf.

6.2 Universal indices of seabed disturbance and sediment mobility

The effectiveness of the oceanographic processes to impact the seabed and to shape benthic habitats depends on both the magnitude of the shear stresses from these processes, and the

frequency with which they occur (Hemer, 2006; Harris, 2012; Li et al., 2015). The mean combined wave-current shear velocity of Figure 15a quantifies only the magnitude of the bed shear stress on the Scotian Shelf and does not reflect the effect of how often shear stresses with various magnitudes occur. For instance, extreme storms tend to produce very high values of shear stress and hence the greatest instantaneous impact on the seafloor. However, these storms occur rarely and last only days and their impact is greatly reduced when the mean bed shear stress is averaged over one or several years. In contrast, the threshold exceedance map of Figure 15c demonstrates how often the combined wave-current shear stress causes mobilization of sediment on the Scotian Shelf, but fails to account for the effect of how strong the mobilization is. Consequently, indices that incorporate both the magnitude and frequency of these processes are needed to better quantify the exposure of the seabed to oceanographic processes and sediment mobilization on continental shelves.

Hemer (2006) proposed three schemes that quantify both the frequency and magnitude of combined-flow bed shear stresses for the regionalization of the Australian continental shelves. However, these schemes did not address the magnitude and frequency of sediment mobilization. Universal indices for seabed disturbance (SDI) and sediment mobility (SMI) considering both the magnitude and frequency have been defined and estimated at both regional scales (Sable Island Bank, Scotian Shelf in Li et al., 2009; the Bay of Fundy in Li et al., 2015) and continental shelf scales (Li et al., 2021a). These indices have also been adopted and applied by international modelling studies (Joshi et al., 2017; Coughlan et al., 2021). More recently, Li et al. (2021b) have applied these indices to quantify the seabed exposure and sediment mobilization on the Canadian Atlantic Shelf using observed grain size data and modelled shear stresses from the full spectrum of wave and current processes.

Following these previous studies, the two universal indices are applied here to quantify the level of seabed exposure to a full range of oceanographic processes and the levels of mobilization of observed sediments on the Scotian Shelf. The Seabed Disturbance Index (SDI) is defined as the maximum value of $\tau_{cws}^{1.5}$ P (Hemer, 2006). Here τ_{cws} is the skin-friction combined wave-current shear stress (= ρu_{*cws}^2) with $\tau_{cws}^{1.5}$ represents the work done by the combined-flow shear stress to disturb the seabed, and P represents the percent time for which a given τ_{cws} value is achieved (i.e. the probability distribution function (PDF) of τ_{cws}). So the product $\tau_{cws}^{1.5}$ P quantifies the level of exposure of the seabed to oceanographic processes, considering both the magnitude and frequency of the combined-flow bed shear stress regardless if sediment mobilization occurs or not. The second parameter Sediment Mobility Index (SMI) is defined as the normalized shear stress (τ_{cws}/τ_{cr}) multiplied by time% of threshold exceedance (i.e. SMF of Figure 15c). The time% of threshold exceedance is the time percent the combined-flow shear stress τ_{cws} exceeds the critical shear stress τ_{cr} for sediment transport initiation. τ_{cws}/τ_{cr} is the mean ratio of τ_{cws} over τ_{cr} for times when τ_{cr} is exceeded. Thus SMI serves as a non-dimensional index

that quantifies the level of sediment mobility integrating both the magnitude and frequency of the sediment mobilization process.

The seabed disturbance index (SDI) map of Figure 17 shows that the highest seabed disturbance up to 1.5 occurs in the upper Bay of Fundy. High SDI values of 0.8 – 1 are found in other areas of Bay of Fundy, on Georges Bank and on western Scotian Shelf. Seabed disturbance is moderate to moderately high (0.2 – 0.5) on the banks of outer Scotian Shelf, in Northeast Channel and along the coast of Nova Scotia. Low disturbance of ~0.1 occurs on LeHave Bank, Emerald Bank, Western Bank on the central Scotian Shelf and in central Gulf of Maine. Seabed disturbance is very low (< 0.03 – 0.04) over western Gulf of Maine and on inner and middle Scotian Shelf. Significant differences in the interpretation of seabed disturbance can be obtained from the SDI map in Figure 17 versus that based on Figure 15a where only the magnitude of combined wave-current shear velocity is used to quantify seabed disturbance. For instance, Figure 15a shows similar moderate shear velocities of 1–2 $cm \cdot s^{-1}$ on eastern Georges Bank and Sable Island Bank implying similar seabed disturbance over these areas. Since Georges Bank is dominated by high-frequency tidal energy while Sable Island Bank is dominated by low-frequency storms (see Figure 16), the use of the SDI map (Figure 17) incorporating both the magnitude and frequency of the shear stress would actually categorize eastern Georges Bank under high disturbance of SDI = 0.6 and Sable Island Bank under moderate disturbance with SDI = 0.3 despite the similar shear velocities.

The spatial distribution of sediment mobility index (SMI) on the Scotian Shelf is shown in Figure 18. High mobility of 1–2 is confined in the upper Bay of Fundy. Moderately high sediment mobility of 0.5–1 is found on Georges Bank, western Scotian Shelf, on the top of Sable Island Bank and along the coast of Nova Scotia. Moderate mobility of 0.05 – 0.3 is predicted on Browns Bank, in Northeast Channel, on Banquereau Bank, and over the remaining areas of Sable Island Bank. Sediment mobility is low at approximately 0.01 – 0.02 on other banks on Scotian Shelf e.g. LeHave Bank, Emerald Bank and Western Bank. Zero sediment mobility is predicted for the Gulf of Maine and the basins on the inner and middle Scotian Shelf. The interpretation of sediment mobility level from the sediment mobility index map of Figure 18 could be quite different than that from the threshold exceedance map of Figure 15c which only considers the mobilization frequency not the magnitude. For instance, the Browns Bank and Sable Island Bank are both classified as areas of high mobility (Figure15c) if only mobilization frequency is considered. The map of mean shear velocity (Figure 15a), however, shows higher combined wave-current shear velocity on Sable Island Bank than Browns Bank. Therefor the SMI values calculated using both the magnitude (represented by the ratio τ_{cws}/τ_{cr}) and frequency of sediment mobilization would classify that sediment mobility on Sable Island Bank is higher than that on Browns Bank (Figure 18).

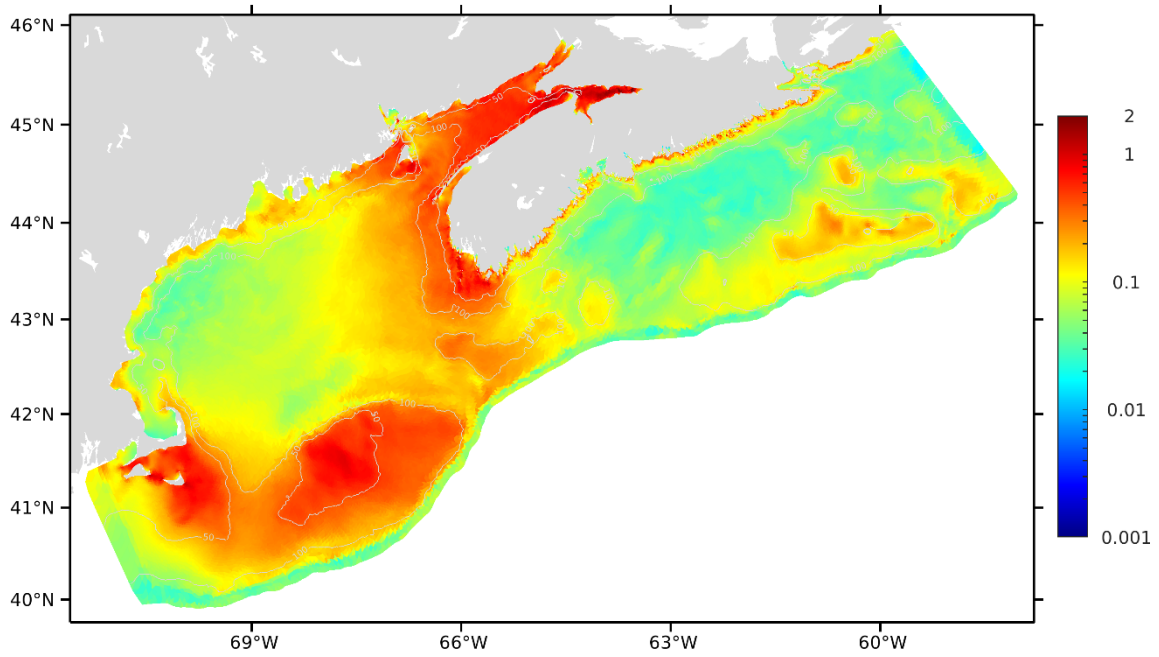

Figure17 Spatial distribution of Seabed Disturbance Index (SDI) on the Scotian Shelf. See text for definition of SDI.

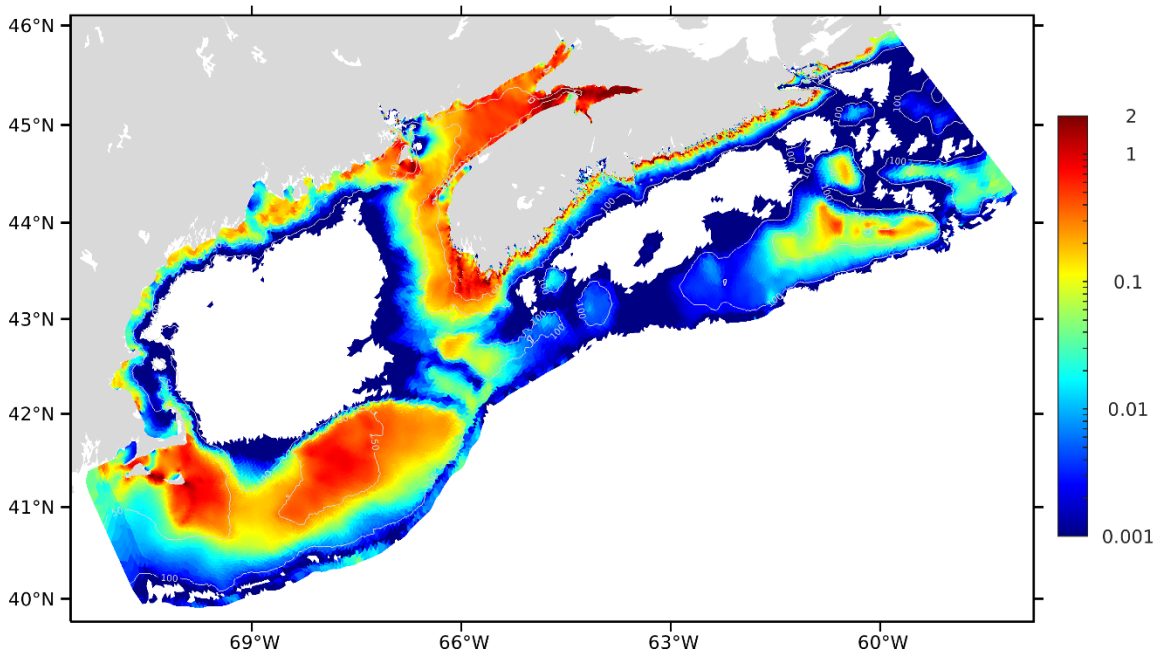

Figure 18 Spatial distribution of Sediment Mobility Index (SMI) on the Scotian Shelf. See text for definition of SMI.

6.3 Advances from previous studies and future efforts

Knowledge on the seabed disturbance and sediment mobilization on the Canadian continental shelves has been achieved progressively through various studies in the last decade. The information of derived parameters, type of grain size data, geographic regions, source data (i.e. oceanographic processes) and computation methods for the present study and those previous studies is summarized in Table 6 to demonstrate the progresses.

6.3.1 Overviews of earlier modelling studies

In developing the benthic habitat map for the Scotian Shelf, Kostylev and Hannah (2007) estimated the disturbance as the ratio of total combined wave-current shear velocity, u_{*cw} (including the effect of bedforms and presence of wave boundary layer), over the critical shear velocity, u_{*cr}, of observed grain size on the Scotian Shelf. This ratio was used as a proxy of the magnitude of sediment mobilization. However it was based on the mean of interpolated near-bed tidal current and 90th percentile of hindcast significant wave height and period, not truly calculated using time series wave and current data. Only wave and tidal processes were considered and processes of ocean circulation current and wind-driven currents in storms were not addressed. The first study addressing the effect of the full range of oceanographic processes was undertaken by Li et al. (2015) who used modelled time series data of waves, tidal currents, wind-driven and circulation currents to predict seabed shear stresses and sediment mobility for observed grain size in the Bay of Fundy. Li et al. (2015) also classified seabed disturbance types and proposed and applied seabed disturbance and sediment mobility indices to quantify the seabed forcing and sediment mobilization incorporating both the magnitude and frequency of these parameters. Although the study of Li et al. (2015) modeled the seabed disturbance and sediment mobility with consideration of the full range of oceanographic processes, it was focused on the Bay of Fundy region and did not represent a shelf-scale study.

In an initial Canada-wide effort, Li et al. (2021a) uses wave hindcast data and modelled depth-averaged tidal current data for a 3-year period to simulate the seabed shear stresses and the mobilization of uniform medium sand on all continental shelves of Canada. The study also undertakes the regionalization of seabed disturbance type and applies the SDI and SMI indices to quantify the seabed exposure to oceanographic processes and sediment mobility incorporating both the magnitude and frequency of these processes. This Canada-wide modelling study thus has established the first national framework of seabed disturbance and sediment mobility on all three continental shelves of Canada. The major limitations of this Canada-wide study are that important ocean circulation and storm-driven current processes were not included and that uniform medium sand instead of observed grain size data was used. The modelling study of Li et al. (2021b) probably represents the most up-to-date and comprehensive shelf-scale study of seabed disturbance and sediment mobilization as it uses time series data of depth-averaged tidal

current, modelled significant wave height and period, near-bed circulation current and storm-induced current to simulate seabed shear stresses, sediment mobilization frequency, disturbance type classification, SDI and SMI of observed grain sizes on the Canadian Atlantic Shelf. The important advances from Li et al., (2021a) are the utility of the full range of oceanographic processes and observed grain size data. The shortcomings of this Atlantic Shelf modelling study are the use of depth-averaged tidal current leading to overestimate of tidal shear stress and sediment mobilization, and the relatively coarse resolution of the current and wave models that limit the application of the modelling results in coastal environments.

6.3.2 Advances and key improvement of the present modelling study

The present study applies the full range of the oceanographic processes and outputs modelled parameters similar to that of Li et al. (2021b). One of the major improvements, however, is the use of near-bottom tidal currents from the 3D current model leading to more realistic values of bed shear stress and sediment mobilization by tidal currents. The higher resolution of the current and wave models used in this study also enhances the applicability of the modelling results to assessing seabed shear stresses and sediment mobility in the nearshore and coastal areas.

The progresses made in various previous modelling studies and the impacts on estimates of bed shear stress and sediment mobilization from the use of time series wave and current data, the inclusion of the full range of oceanographic processes, and the use of observed grain size versus uniform sediment have been described in detail in Li et al. (2021b). Since the use of near-bottom tidal currents is one of the major improvements of the present study from previous works, we further explore the differences of the modelled tidal currents and how these affect sediment mobilization frequency and disturbance type classification on the Scotian Shelf. Comparison between modelled near-bottom tidal currents shown in Figure 8 with the modelled depth-averaged tidal currents of Li et al. (2021b) (Figure 19a) demonstrates that the modelled near-bottom tidal currents are moderately lower than the depth-averaged tidal currents. The mean depth-averaged tidal current speeds reach 0.8 m/s on Georges Bank and on the shelf off southwestern Nova Scotia while the modelled near-bottom tidal currents (Figure 8) only reach 0.5 m/s over these areas. Over the banks on the outer Scotian Shelf, depth-averaged tidal currents were moderate with speeds of 0.3–0.4 $m \cdot s^{-1}$. The speed of the near bottom tidal currents over these banks decrease to 0.2 – 0.3 m/s. The lower near-bottom tidal current speeds are translated to reduced sediment mobilization frequency by tidal currents on the Scotian Shelf. Sediment mobilization frequency predicted using depth-averaged tidal currents was up to 100% of the time in the Bay of Fundy, on Georges Bank, and on the shelf off southwestern Nova Scotia (Figure 19b). The maximum mobilization frequency of 100% of the time is only predicted for Georges

Table 6 Summary of derived parameters, grain size data, geographic region, source data (oceanographic processes) and computation method of Canadian seabed disturbance studies.

Studies	Parameters, grain size and region	Source data and calculation method
Kostylev and Hannah (2007)	Total shear velocity u_{*cw}; disturbance defined as ratio of u_{*cw} over critical shear velocity u_{*cr}; Observed grain size; Scotian Shelf	Total u_{*cw} calculated from RMS near-bed tidal current extrapolated from 2D model and 90^{th} percentile of hindcast wave height and period data; SEDTRANS model; Not based on time series data of current and wave.
Li et al. (2015)	Skin-friction seabed shear stresses, sediment mobilization frequency, disturbance type classification, seabed disturbance index and sediment mobility index; observed grain size; Bay of Fundy region	Time series data of wave height and period and depth-averaged tidal current, circulation current and storm-induced current; SEDTRANS model
Li et al. (2021a)	Skin-friction seabed shear stresses, sediment mobilization frequency, disturbance type classification, seabed disturbance index and sediment mobility index; uniform medium sand; All three shelves of Canada	Time series data of depth-averaged tidal current; wave height and period extracted from public domains; circulation and storm-induced currents not included; SEDTRANS model
Li et al. (2021b)	Skin-friction seabed shear stresses, sediment mobilization frequency, disturbance type classification, seabed disturbance index and sediment mobility index; observed grain size; Canadian Atlantic Shelf	Time series data of depth-averaged tidal current, modelled wave height and period data, near-bed circulation current and storm-induced current; SEDTRANS model
This study	Skin-friction seabed shear stresses, sediment mobilization frequency, disturbance type classification, seabed disturbance index and sediment mobility index; updated observed grain size; Scotian Shelf Bioregion	High resolution time series data of near-bed tidal, circulation and storm-induced current; high-resolution modelled wave height and period data; ROMS sediment module

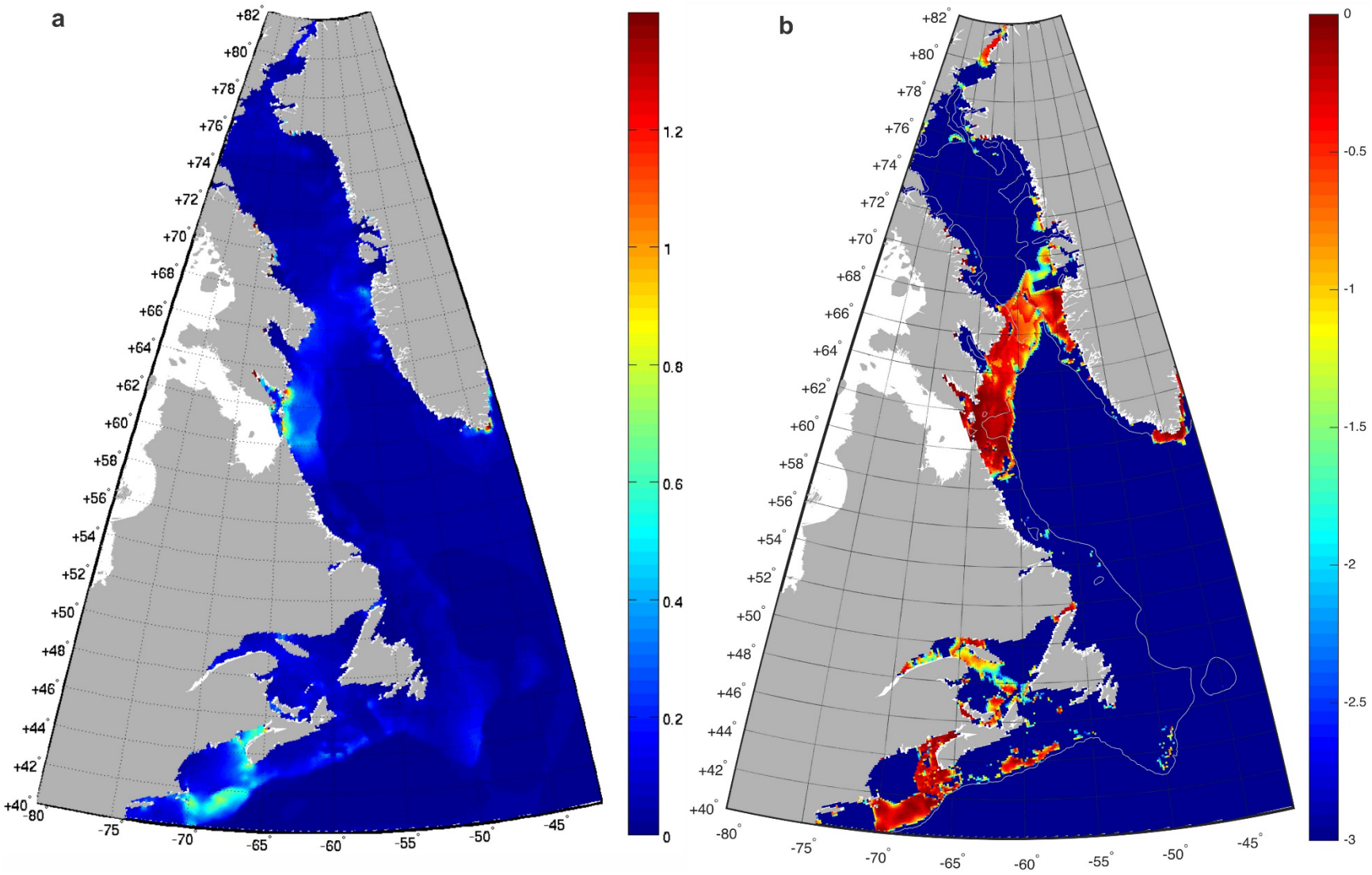

Figure 19 Spatial distribution of (a) mean depth-averaged tidal current speed (m s^{-1}) and (b) sediment mobilization frequency (% of time) by tidal current on the Atlantic Shelf (from Li et al., 2021b).

Bank based on near-bottom tidal current (Figure 13c) and sediment mobilization frequencies reached only 50−80% of the time in the Bay of Fundy and on the shelf off southwestern Nova Scotia. On the outer shelf banks, sediment mobilization frequency based on depth-averaged tidal currents was 50−70% of the time. These values based on near-bottom tidal currents decrease to 20−30% of the time on these outer shelf banks.

As described in Section 6.1, the use of the lower modelled near-bottom tidal currents also affect the disturbance type distribution on the Scotian Shelf. The disturbance type classification of Li et al. (2021b) using depth-averaged tidal currents categorizes the disturbance on Scotian Shelf as predominantly tide dominant while the present modelling study using near-bottom tidal currents indicates the area of wave dominant disturbance to be double that of tide dominant type. Also the higher depth-averaged tidal currents used in Li et al. (2021b) classifies the Georges Bank and the shelf off southwestern Nova Scotia as entirely tide dominant type while the present study using lower near-bottom tidal currents shows that significant parts of these areas are actually under wave dominant and mixed disturbance types.

The improved knowledge on dominant processes and quantification of the magnitude and frequency of seabed shear stress and sediment mobilization on the Scotian Shelf from this modelling study should facilitate seabed stability evaluation for offshore renewable energy development (Németh et al., 2003; Barrie and Conway, 2014; Roetert et al., 2017; and Eamer et al., 2021) and contribute to understanding habitat distribution and dynamics (Kostylev and Hannah, 2007 and King et al., 2021) on the Scotian Shelf.

6.3.3 Areas for future efforts

In developing the initial Canada-wide framework of seabed disturbance and sediment mobility, Li et al. (2021a) have identified several areas for improvement in future modelling studies. The most important areas are the addition of storm-induced current and background circulation current processes, the use of near-bottom currents from three-dimensional current models and modelling shear stress and sediment mobilization based on observed grain size data. Li et al. (2021b) has made substantive advances to address these areas by including ocean circulation currents and storm-induced currents and using observed grain size to model the seabed disturbance and sediment mobility for the Canadian Atlantic Shelf. The present modelling study has made further progress by using near-bottom tidal currents and applying higher resolution current and wave models. There are still areas that future seabed disturbance modelling research can be improved. There are poor or no coverage of observed grain size data in areas of the north Atlantic Shelf, on the Northeast Newfoundland Shelf, and on the Grand Banks. Efforts should be made to collect seabed samples over these areas and the improved grain size data integrating all possibly available sample data should be used in future modelling studies. Energetic events such as temperate storms and cyclones or hurricanes occur on time

scales of days to years. Future modelling studies in Canada need to make efforts to model seabed stresses and sediment mobilization for longer time durations. Stratification of water column on the continental shelf can substantially modify the vertical structure of the tidal currents due to the generation of internal tides over steep topography (e.g. Cummins and Oey, 1997) or amplify tidal currents and cause episodic erosion and transport of sediments in canyons and on the shelf edge (Li et al., 2019). Future seabed disturbance modelling should consider including the internal tides in the modelled oceanographic processes.

7. Conclusions

A newly developed high resolution 3-D current model, a high-resolution coastal wave model, and a widely applied sediment transport module have been applied to provide the latest spatial estimates of bed shear stresses and mobilization of observed sediments on the Scotian Shelf for the three year period of 2017 – 2019. The present study has advanced previous shelf-scale modelling studies by utility of modelled near-bottom tidal currents, high resolution nearshore focused wave model, and a new sediment module with the added potential of modelling sediment transport pathways.

The Scotian Shelf is affected by strong waves and tidal currents. Maximum mean significant wave height can reach 2.4 m and maximum mean tidal currents can reach 0.5 $m \cdot s^{-1}$. Circulation and storm-driven currents add additional 0.2 $m \cdot s^{-1}$ speed. These waves, currents and/or their interaction cause maximum mean bed shear velocities of 5 – 10 $cm \cdot s^{-1}$ that predominantly occur in the Bay of Fundy, on Georges Bank, and on the shelf off southwestern Nova Scotia. Our modelling results suggest that tidal currents alone are capable to mobilize sediments at least once during the modelled 3 year period over 28% of the shelf area while waves can cause sediment mobility over 60% of the shelf area suggesting much stronger effect of waves. Interaction between waves and currents can produce enhanced combined wave-current shear velocity that is capable to mobilize sediments over 74% of the shelf area.

The seabed disturbance type classification based on the relative mobilization frequency of component processes on the Scotian Shelf suggests that wave dominant disturbance is predominant accounting for 38.2% of the shelf area and mainly occurs on central and eastern Scotian Shelf and along the coasts of Scotian Shelf. Tide dominant disturbance type is second important to account for 19.1% of the shelf area and mainly occurs in the Bay of Fundy, on Georges Bank and on western Scotian Shelf. The present modelling study using near-bed tidal currents and new modelled waves demonstrates the area of wave dominant disturbance to be double that of tide dominant type in contrary to the finding that the disturbance on Scotian Shelf is predominantly tide dominant from the modelling study for the Atlantic Shelf (Li et al., 2021b). The use of near-bottom tidal currents has also resulted in reduced sediment mobilization frequency by tidal currents, smaller extent of high mobility areas and significant changes of the spatial pattern of disturbance type distribution on the Scotian Shelf.

The universal Seabed Disturbance Index (SDI) and Sediment Mobility Index (SMI) have been applied to better quantify the seabed exposure to physical processes and sediment mobilization on the Scotian Shelf by accounting for both the magnitude and frequency of these processes. The applications of these indices are shown to provide improved quantification of seabed forcing and sediment mobility for several areas on the Scotian Shelf. The improved knowledge on dominant processes and the magnitude and frequency of seabed shear stress and sediment mobilization on the Scotian Shelf from this study should facilitate seabed stability evaluation for offshore renewable energy development and contribute to understanding the habitat distribution and dynamics on the Scotian Shelf.

Acknowledgement

We would like to thank Vladimir Kostylev, Calvin Campbell and Gary Sonnichsen for their scientific support of this research Activity as part of the GSC MGMSP program. We are thankful to Kate Jarret, Owen Brown and Emily Maclean for help with grain size data compilation and analysis. Paul Hill of Dalhousie University and Tim Milligan of DFO kindly shared additional compiled GSC and USGS grain size data for the Bay of Fundy and Gulf of Maine region. We also thank Tao Feng of DFO for his work of the FVCOM model setup and model run. Internal review by Jordan Eamer substantially improved the quality of this report.

References

Amos, C.L., Brylinsky, M., Lee, S., O'Brien, D., 1996. Littoral mudflat stability monitoring the Humber estuary, S. Yorkshire, England LISPUK, April, 1995. Geological Survey of Canada Open File 3214. 46pp.

Amos, C.L., Feeney, T., Sutherland, T.F. and Luternauer, J.L., 1997. The stability of fine-grained sediments from the Fraser River Delta, ECSS, 45: 507-524.

Ariathurai, C.R., Arulanandan, K., 1978. Erosion rates of cohesive soils. Journal of the Hydraulics Division 104, 279–282.

Barrie, J.V. and Conway, K.W., 2014. Seabed characterization for the development of marine renewable energy on the Pacific margin of Canada. Continental Shelf Research 83, 45–52; http://dx.doi.org/10.1016/j.csr.2013.10.016

Bever, A.J. and Harris, C.K., 2014. Storm and fair-weather driven sediment-transport within Poverty Bay, New Zealand, evaluated using coupled numerical models. Continental Shelf Research, 86, 34-51.

Blaas, M., Dong, C., Marchesiello, P., McWilliams, J. C., & Stolzenbach, K. D., 2007. Sediment-transport modeling on Southern Californian shelves: A ROMS case study. Continental Shelf Research 27: 832-853.

Cacchione, D.A. and Drake, D.E., 1990. Shelf sediment transport: An overview with applications to the Northern California continental shelf. In: The Sea, Vol.9, B. Le Mehaute and D.M. Hanes, (eds.), Wiley Interscience, pp. 729-773.

Chen, C., Liu, H., & Beardsley, R. C., 2003. An unstructured grid, finite-volume, three-dimensional, primitive equations ocean model: Application to coastal ocean and estuaries. Journal of Atmospheric and Oceanic Technology, 20, 159–186. https://doi.org/10.1175/1520-0426(2003)020<0159:augfvt>2.0.co;2

Connor, D.W., Allen, J.H., Golding, N., Howell, K.L., Lieberknecht, L.M., Northen, K.O. and Reker, J.B., 2004. Marine habitat classification for Britain and Ireland Version 04.05, Joint Nature Conservation Committee, Peterborough UK. www.jncc.gov.uk/page 1645.

Coughlan M., Guerrini M., Creane S., O'Shea M., Ward S.L., Van Landeghem K.J.J., Murphy J., Doherty P., 2021. A new seabed mobility index for the Irish Sea: Modelling seabed shear stress and classifying sediment mobilisation to help predict erosion, deposition, and sediment distribution. CSR, 229, (2021) 104574. https://doi.org/10.1016/j.csr.2021.104574

Cummins, P.F. and Oey, L.Y. 1997. Simulation of barotropic and baroclinic tides off northern British Columbia. Journal of Physical Oceanography, 27: 762-81.

Dickhudt, P.J., Friedrichs, C.T., Sanford, L.P., 2011. Mud matrix solids fraction and bed erodibility in the York River estuary, USA, and other muddy environments. Continental Shelf Research 31, S3–S13.

Eamer. J.B.R., Shaw, J., King, E.L., MacKillop, K., 2021. The inner shelf geology of Atlantic Canada compared with the North Sea and Atlantic United States: Insights for Atlantic Canadian offshore wind energy. Continental Shelf Research, 213, 104297. https://doi.org/10.1016/j.csr.2020.104297.

Fader, G.B.J. 1991. Surficial geology and physical properties 5: Surficial Geology. in: Ross, D. I., Lewis, C.F.M., Howie, R.D., Cant, D., Bates, J.L. (eds.), Geological Survey of Canada, East Coast Basin Atlas Series: Scotian Shelf, 1991; p. 119; 1 sheet, doi:10.4095/210696.

Feng, T., Stanley, R. R. E., Wu, Y., Kenchington, E., Xu, J., & Horne, E. 2022. A High-resolution 3-D circulation model in a complex archipelago on the coastal Scotian Shelf. Journal of Geophysical Research: Oceans, 127, e2021JC017791. https://doi.org/10.1029/2021JC017791

Fisheries and Oceans Canada, 2009. Development of a framework and principles for the biogeographic classification of Canadian marine areas; Canadian Science Advisory Secretariat, Science Advisory Report 2009/056, 17 p.

Garrett, C., 1972. Tidal resonance in the Bay of Fundy and Gulf of Maine. Nature, 238, 441–443. doi:10.1038/238441a0.

Gibbs, R. J., Mathews, M. D., and Link, D. A., 1971, The relationship between sphere size and settling velocity. Jour. Sed. Pet., 41, p. 7-18.

Gregr, E.J., R. Gryba, M. Z. Li, H. Alidina, V. Kostylev, and C.G. Hannah. 2016. A benthic habitat template for Pacific Canada's continental shelf. Can. Tech. Rep. Hydrogr. Ocean Sci. 312: vii + 37 p. https://waves-vagues.dfo-mpo.gc.ca/Library/40566389.pdf

Gust, G., Morris, M.J., 1989. Erosion thresholds and entrainment rates of undisturbed in-situ sediments. Journal of Coastal Research (Special Issue) 5, 87–100.

Harris, C.K., Wiberg, P.L., 1997. Approaches to quantifying long-term continental shelf sediment transport with an example from the Northern California STRESS mid-shelf site. Continental Shelf Research 17, 1389–1418.

Harris, C.K., Wiberg, P.L., 2001. A two-dimensional, time dependent model of suspended sediment transport and bed reworking for continental shelves. Computers & Geosciences 27, 675–690.

Harris, C. K., C. R. Sherwood, R. P. Signell, A. J. Bever, and J. C. Warner, 2008. Sediment dispersal in the northwestern Adriatic Sea, J. Geophys. Res., 113, C11S03, doi:10.1029/2006JC003868.*

Harris, P.T., 2012. On seabed disturbance, marine ecological succession and applications for environmental management: a physical sedimentological perspective. In: Li, M., Sherwood, C., Hill, P. (Eds.), Sediments, Morphology and Sedimentary Processes on Continental Shelves. International Association of Sedimentologists Special Publication, 44, pp. 387–404 (Oxford).

Harris, P.T., Coleman, R., 1998. Estimating global shelf sediment mobility due to swell waves. Mar. Geol. 150, 171– 177.

Harris, P.T. and Hughes, M.G., 2012. Predicted benthic disturbance regimes on the Australian continental shelf: a modelling approach. Marine Ecology Progress Series, 449: 13-25.

Hemer, M., 2006. The magnitude and frequency of combined flow bed shear stress as a measure of exposure on the Australian continental shelf. Continental Shelf Research, 26, 1258-1280.

Joshi, S., Duffy, G.P., Brown, C., 2017. Mobility of maerl-siliciclastic mixtures: impact of waves, currents and storm events. Estuar. Coast Shelf Sci. 189, 173–188. https://doi. org/10.1016/j.ecss.2017.03.018.

Katavouta, A., Thompson, K. R., Lu, Y., & Loder, J. W., 2016. Interaction between the tidal and seasonal variability of the Gulf of Maine and Scotian shelf region. Journal of Physical Oceanography, 46, 3279–3298. https://doi.org/10.1175/JPO-D-15-0091.1

King, M., Koropatnick, T., Gerhartz Abraham, A., Pardy, G., Serdynska, A., Will, E., Breeze, H., Bundy, A., Edmondson, E., and Allard, K. 2021. Design Strategies for the Scotian Shelf Bioregional Marine Protected Area Network. DFO Can. Sci. Advis. Sec. Res. Doc. 2019/067. vi + 122 p.

Kostylev, V.E. and Hannah, C.G., 2007 . Process Driven Characterization and Mapping of Seabed Habitats. In: Todd, B.J., and Greene, H.G., eds., Mapping the Seafloor for Habitat Characterization: Geological Association of Canada, Special Paper 47, p. 171-184.

Li, M.Z. and Amos, C.L., 2001. SEDTRANS96: the upgraded and better calibrated sediment transport model for continental shelves. Computers and Geosciences, 27, 619-645.

Li, M.Z., Parrott, D. R. and Yang, Z., 2009. Sediment Stability and Dispersion at the Black Point Offshore Disposal Site, Saint John Harbour, New Brunswick, Canada. Journal of Coastal Research, 25: 1025 - 1040.

Li, M. Z., King, E.L. and Prescott, R.H., 2012. Seabed disturbance and bedform distribution and mobility on the storm-dominated Sable Island Bank, Scotian Shelf. In: Sediments, Morphology and Sedimentary Processes on Continental Shelves, Li, M.Z., Sherwood, C. and Hill, P. (Eds.), Special Publication 44 of the International Association of Sedimentologists, Wiley-Blackwell, 197–227.

Li, M. Z., Hannah, C.G., Perrie, W.A., Tang, C.C.L., Prescott, R.H. and Greenberg, D.A., 2015. Modelling Seabed Shear Stress, Sediment Mobility and Sediment Transport in the Bay of Fundy. Canadian Journal of Earth Sciences, 52, 757-775; 10.1139/cjes-2014-0211.

Li, M.Z., Prescott, R.H. and Robertson, A.G. 2019. Observation of internal tides and sediment transport processes at the head of Logan Canyon on central Scotian Slope, eastern Canada. Journal of Marine Systems, 193: 103–125.

Li, M.Z., Wu, Y., Hannah, C.G. and Perrie, W.A., 2021a. Seabed disturbance and sediment mobility due to tidal current and waves on the continental shelves of Canada. Can. J. Earth Sci. 58, 1209–1232; dx.doi.org/10.1139/cjes-2020-0139

Li, M.Z., Wu, Y., Hannah, C.G., Perrie, W.A., Shen, H., and King, E.L., 2021b. Modelling seabed disturbance and sediment mobility on the Canadian Atlantic Shelf; Geological Survey of Canada, Open File 8805, 50 p. https://doi.org/10.4095/328363

Long, B.F.N., 1979. The nature of bottom sediments in the Minas Basin system, Bay of Fundy. Bedford Institute of Oceanography Data series, BI-D-79-4, 101 p.

Lyard, F. H., Carrère, L., Cancet, M., Boy, J., & Gégout, P., 2016. The FES2014 tidal atlas, accuracy assessment for satellite altimetry and other geophysical applications. EGU General Assembly Conference Abstracts, 18, 17693.

Madsen, O.S., 1994. Spectral wave–current bottom boundary layer flows. In: Coastal Engineering 1994. Proceedings of the 24th International Conference on Coastal Engineering Research Council, Kobe, Japan, pp. 384–398.

Miller, M.C., McCave, I.N., and Komar, P.D., 1977. Threshold of sediment motion under unidirectional currents. Sedimentology, 24, 507-527.

Németh, A. A., Hulscher, S. J. M. H., & de Vriend, H. J., 2003. Offshore sand wave dynamics, engineering problems and future solutions. Pipeline and Gas Journal, 230(4), 67.

Nittrouer, C.A. and Wright, L.D., 1994. Transport of particles across continental shelves. Reviews of Geophysics, 32: 85-113.

Piper, D.J.W. 1991. Seabed geology of the Canadian eastern continental shelf. Continental Shelf Research, 11: 1013-1035.

Poppe, L.J., McMullen, K.Y., Williams, S.J., and Paskevich, V.F., eds., 2014, USGS east-coast sediment analysis: Procedures, database, and GIS data (ver. 3.0, November 2014): U.S. Geological Survey Open-File Report 2005-1001, https://woodshole.er.usgs.gov/openfile/of2005-1001/

Porter-Smith, R., Harris, P.T., Andersen, O.B., Coleman, R., Greenslade, D., Jenkins, C.J., 2004. Classification of the Australian continental shelf based on predicted sediment threshold exceedance from tidal currents and swell waves. Marine Geology, 211, 1–20.

Praeg, D., MacLean, B., and Sonnichsen, G., 2007. Quaternary Geology of the Northeast Baffin Island Continental Shelf, Cape Aston to Buchan Gulf (70º to 72ºN); Geological Survey of Canada, Open File 5409, 1 CD-ROM.

Reid, J.M., Reid, J.A., Jenkins, C.J., Hastings, M.E., Williams, S.J., and Poppe, L.J, 2005. usSEABED: Atlantic coast offshore surficial sediment data release: U.S. Geological Survey Data Series 118, version 1.0. https://pubs.usgs.gov/ds/2005/118/

Roetert, T., Raaijmakers, T., & Borsje, B., 2017. Cable route optimization for offshore wind farms in Morphodynamic areas. Paper presented at the 27th. International Ocean and Polar Engineering Conference.

Shaw, J., Todd, B.J. and Li, M.Z. 2012. Seascapes, Bay of Fundy, offshore Nova Scotia/New Brunswick. Geological Survey of Canada, Open File 7028.

Shaw, J., Todd, B.J. and Li, M.Z. 2014. Geologic insights from multibeam bathymetry and seascape maps of the Bay of Fundy, Canada. Continental Shelf Research, 83: 53-63.

Shaw, J., Todd, B.J., Li, M.Z., Mosher, D.C., and Kostylev, V.E., 2014. Continental Shelves of Atlantic Canada. In: Chiocci, F. L. & Chivas, A. R. (eds) 2014. Continental Shelves of the World: Their Evolution During the Last Glacio-Eustatic Cycle. Geological Society London, Memoirs, 41, 7–19.

Sherwood, C.R., Aretxabaleta, A.L., Harris, C.K., Rinehimer, J.P., Verney, R. and Ferré, B., 2018. Cohesive and mixed sediment in the Regional Ocean Modeling System (ROMS v3.6) implemented in the Coupled Ocean–Atmosphere–Wave–Sediment Transport Modeling System (COAWST r1234). Geosci. Model Dev., 11, 1849–1871; https://doi.org/10.5194/gmd-11-1849-2018

Shields, A., 1936. Anwendung der Aehnlichkeitsmechanik und der Turbulenz- forschung auf die Geschiebebewegung, Mitt. Preuss. Versuchsanst. Wasserbau Schiffbau (English translation by Ott, W.P., van Uchelen J.C., U.S. Department of Agricultural, Soil Conservation Service Cooperative Laboratory, California Insti- tute of Technology, Pasadena, 1936, 36 pp.).

Soulsby, R.L., Damgaard, J.S., 2005. Bedload sediment transport in coastal waters. Coastal Engineering 52 (8), 673–689.

Swift, D.J.P., Han, G., Vincent, C.E., 1986. Fluid processes and sea-floor response on a modern storm-dominated shelf: Middle Atlantic shelf of north America: Part 1. The storm-current regime. In: Knight, R.J., McLean, J.R. (Eds.), Shelf Sands and Sandstones. Canadian Society of Petroleum Geologists, Calgary, pp. 99–119.

Walker, R.G., 1984. Shelf and shallow marine sands. In: Walker, R.G. (Ed.), Facies Models. Geological Association of Canada, Toronto, pp. 141– 170.

Warner, J. C., Sherwood, C., Signell, R.P., Harris, C.K. and Arango, H.G., 2008a. Development of a three-dimensional, regional, coupled wave, current, and sediment-transport model, Comput. Geosci., 34, 1284– 1306.

Warner, J. C., Butman, B., & Dalyander, P. S., 2008b. Storm-driven sediment transport in Massachusetts Bay. Continental Shelf Research 28: 257-282.

Wiberg, P.L., Harris, C.K., 1994. Ripple geometry in wave dominated environments. Journal of Geophysical Research 99 (C1), 775–789.

Willmott, C. J., 1981. On the validation of models. Physical Geography, 2(222), 184–194. https://doi.org/10.1080/02723646.1981.10642213

Appendices

Appendix 1 Grain size data from analysis of legacy samples in the Baffin Bay undertaken in the 2014−2018 efforts. sub_top – top of subsample in cm from sediment surface; sub_bot - bottom of subsample in cm from sediment surface.

Appendix 2 Grain size data for the Bay of Fundy digitized from Long (1979) and for Baffin Bay digitized from GSC Open File 5409 (Praeg et al., 2007). OF_sample# gives the sample# used in Open File 5409. Definition of other columns is the same as Appendix 1.

Appendix 3 Grain size data for the Bay of Fundy collected by DFO in the years 1977 and 1994 (Tim Milligan and Paul Hill, personal communication). Definition of columns is the same as Appendix 1.